

“WIND ANALYSIS OF CABLE-STAYED BRIDGE AND ITS MITIGATION MEASURES”

A Dissertation submitted in partial fulfillment of the requirement for the
Award of degree of

**MASTER OF TECHNOLOGY
IN
STRUCTURAL ENGINEERING**

By

RITU RAJ

Roll No. – 2K14/STE/13

Under the esteemed guidance of

Dr. Nirendra Dev

(Professor)

Head of Department, Civil Engineering



**Department of Civil Engineering
Delhi Technological University
(FORMERLY DELHI COLLEGE OF ENGINEERING)**

JUNE 2016

CERTIFICATE

*This is to certify that the dissertation entitled “**Wind Analysis Of Cable- Stayed Bridge And Its Mitigation Measures** ” is being submitted by me, **Ritu Raj** bearing roll no. **2K14/STE/13** to the **Delhi Technological University, New Delhi**, for the degree of Master of Technology in **Structural Engineering**, run by Civil Engineering Department is a bonafide work carried out by me. The research reports and the results presented in this thesis have not been submitted in parts or in full to any other University or Institute for the award of any degree.*

Ritu Raj

(Candidate)

Department of Civil Engineering

Delhi Technological University

This is to certify that the above statement made by the candidate is true to the best of my knowledge and belief.

Dr. Nirendra Dev

(Supervisor)

Professor

Head of Department

Department of Civil Engineering

Delhi Technological University, New Delhi (India)

ACKNOWLEDGEMENT

I wish to express my sincere gratitude to *Dr. Nirendra Dev*, Professor and Head of Department of Civil Engineering, Delhi Technological University, New Delhi, who has graciously provided me his valuable time whenever I required his assistance. His counselling, supervision and suggestions were always encouraging and it motivated me to complete the project at hand.

At many stages in the course of this research project I benefited from his advice, particularly when exploring new ideas. His positive outlook and confidence in my research inspired me and gives me confidence. He will always be regarded as a great mentor for me.

I would like to express my heartiest thank to my friends and seniors for constant support and motivation. I would like to thank the Department of Civil Engineering, for providing us with the facilities of laboratory, faculty members and all staff members. Last but not least I thank my parents, for everything I am and will be in future. It's your unspoken prayers and affection that keep me moving forward.

RITU RAJ

Roll No.: 2K14/STE/13

Department of Civil Engineering

Delhi Technological University

ABSTRACT

The intent of this research is to present a detailed study of various phenomenons' that induce vibrations in Cable-stayed bridges. The wind load analysis is carried out for a Cable-stayed bridge model for Indian terrain conditions. The wind load analysis is carried out on MIDAS CIVIL 2012 to check the behavior of bridge vulnerability against wind forces.

It involves the determination of natural frequency of stay cables and profile of the cable under axial tension and self weight of the cable. The dynamic characteristics of a structure can be effectively analyzed in terms of natural modes of vibrations i.e. in terms of natural frequencies and mode shapes. As the model is a 3D Finite element model, a general modal analysis capable to provide all possible modes of the bridge (transverse, vertical, torsion and coupled).

As the second part of work appropriate counter measures to mitigate the oscillations are described in this chapter. These counter measures can be implemented at the source, in such a way that the generation of vibration is limited, or at the structure, through the installation of control systems that have the effect of limiting the response.

TABLE OF CONTENTS

TABLE OF CONTENTS.....	I
LIST OF FIGURES AND TABLES	IV
CHAPTER 1	1
INTRODUCTION	1
1.1 GENERAL	1
1.2 NECESSITY OF WIND LOAD ANALYSIS FOR CABLE-STAYED BRIDGES.....	1
1.3 SCOPE OF WORK:.....	2
1.4. LAYOUT OF THE DISSERTATION.....	3
CHAPTER 2.....	4
LITERATURE REVIEW.....	4
2.1. GENERAL.....	4
2.2. HISTORICAL DEVELOPMENTS.....	4
2.3. ANALYTICAL WORK.....	4
2.4. EXPERIMENTAL WORK.....	7
3.1.INTRODUCTION TO CABLE STAYED BRIDGE.....	9
3.2.1.ARRANGEMENT OF THE STAY CABLES.....	10
3.2.2.SELECTION OF CABLE CONFIGURATION	11
3.2.3.POSITIONS OF THE CABLES IN SPACE	12
3.2.3.1. <i>The Two Planes System</i>	12
3.2.3.2. <i>The Single Plane System</i>	13
3.2.4. TOWER (OR PYLON) TYPES	14
3.2.5. DECK TYPES.....	15
3.2.6. MAIN GIRDER	16
3.2.6 CABLE TYPES	17
3.3. WIND LOADING IN STAY CABLES.....	18
3.4.1. GENERAL	18
3.4.1.2. <i>Fixed cylinder immersed in turbulent flow</i>	25
3.4.1.3. <i>Moving cylinder immersed in turbulent flow</i>	27
3.4.1.4. <i>Linearised equation of motion</i>	29
3.5. VIBRATION PHENOMENON DIRECTLY INDUCED BY WIND.....	31

3.5.1. VORTEX-SHEDDING	31
3.5.2. BUFFETING.....	32
3.5.3. GALLOPING	33
3.5.4. FLUTTER	36
3.5.5. WAKE EFFECTS	37
3.5.5.1. Resonant buffeting.....	38
3.5.5.2. Vortex resonance	38
3.5.5.3. Interference effects	39
3.6. RAIN-WIND INDUCED VIBRATIONS.....	40
3.7. DRAG CRISIS.....	41
3.8. INDIRECT EXCITATION.....	41
CHAPTER 4.....	42
MODELLING AND ANALYSIS.....	42
4.1. GENERAL.....	42
4.2. NONLINEARITIES OF CABLE STAYED BRIDGE	42
4.2.1. BEAM – COLUMN EFFECT	42
4.2.2. CABLE SAG EFFECT.....	43
4.3. CABLE-STAYED BRIDGE MODEL	44
4.3.1. GENERAL ARRANGEMENT:	44
4.3.2. STRUCTURAL ANALYSIS SOFTWARE:	45
4.3.3. MATERIAL:.....	45
4.4. STATIC ANALYSIS.....	46
4.5. DYNAMIC ANALYSIS	48
4.6. CALCULATION OF WIND LOAD	48
4.7. WIND ANALYSIS RESULTS.....	55
CHAPTER 5.....	56
MITIGATION MEASURES FOR WIND INDUCED VIBRATIONS IN	56
CABLE-STAYED BRIDGES	56
5.1. INTRODUCTION.....	56
5.2. VIBRATION CONTROL SYSTEMS	56
5.2.1. AERODYNAMIC CONTROL OF VIBRATIONS	56
5.2.2. STRUCTURAL CONTROL OF VIBRATIONS	58

5.2.3. MECHANICAL CONTROL OF VIBRATIONS..... 59

5.2.4. ACTIVE CONTROL SYSTEM..... 63

 5.2.4.1. *Active aerodynamic appendages* 64

 5.2.4.2. *Active tendon control*..... 64

 5.2.4.3. *Active mass dampers* 65

5.3. SUMMARY 65

CHAPTER 6..... 66

SUMMARY AND CONCLUSION 66

6.1. SUMMARY 66

6.2. CONCLUSIONS..... 67

6.2. FUTURE SCOPE OF WORK..... 68

REFERENCES..... 69

LIST OF FIGURES AND TABLES

Figure 3.1	Behaviour of Cable-stayed Bridge.	9
Figure 3.2	Arrangement of Stay Cables.	11
Figure 3.3	Various basic tower shapes.	14
Figure 3.4	Shapes of Girders.	16
Figure 3.5	Various cable patterns.	17
Figure 3.6	A classification of flow-induced vibrations.	18
Figure 3.7	Fixed rigid cylinder of infinite length immersed in a smooth flow: (a) Reference Cartesian systems and wind velocity field; (b) aerodynamic forces.	20
Figure 3.8	Flow past circular cylinder.	22
Figure 3.9	Variation of CD with Re for a circular cylinder	23
Figure 3.10	Fixed cylinder of Infinite length immersed in turbulent flow: (a) Reference Cartesian system and wind velocity field; (b) aerodynamic forces.	25
Figure 3.11	Moving cylinder of Infinite length immersed in turbulent flow: (a) Reference Cartesian system and wind velocity field; (b) aerodynamic forces.	27
Figure 3.12	Vortex shedding behind a circular cylinder.	31
Figure 3.13	Lift and Drag forces on a fixed bluff object.	34
Figure 3.14	Effective angle of attack on an oscillating bluff body.	35
Figure 3.15	Action of gust on the two planes of stays.	38
Figure 3.16	Vortex shedding in the wake of a bridge pylon.	39
Figure 4.1	Isometric View of the Model	44
Figure 4.2	Deflection (Dead Load).	47
Figure 4.3	Bending Moment Diagram (Dead Load).	47
Figure 4.4	1 st Mode Shape- Vertical and Transverse Mode.	48
Figure 4.5	Geometry of Cable-Stayed Bridge Model	50
Figure 5.1	(a) – Examples of aerodynamic appendages for a bridge deck. (b) -Examples of aerodynamic control of vibration for bridge towers	57
Figure 5.2	Add-on devices for suppression of vortex-induced vibrations: a) Helical Stake b) Shroud c) axial slats d) streamlined fairing e) splitter f) ribboned g) pivoted guiding vane h) spoiler plate	58
Figure 5.3	Scheme of cross-cable systems installed some bridges.	59
Figure 5.4	(a) TMD of Normandy bridge, scheme and photograph.	60
Figure 5.4	(b) Location and scheme of TMDs installed at the towers of Yokhama Bay bridge.	60
Figure 5.5	(a) Hydraulic damper at Iroise.	61
Figure 5.5	(b) Hydraulic damper at Aratsu bridge.	61
Figure 5.6	Scheme of Ring Damper.	62

Figure 5.7	Internal damper installed on a stay cable of Vasco da Gama bridge.	63
Table 4.1	Material Properties	46
Table 4.2	Maximum Responses.	46
Table 4.3	Natural Frequencies and Mode shapes.	49
Table 4.4	Maximum Responses.	53

Chapter 1

INTRODUCTION

1.1 General

In the last several decades, cable-stayed bridges have become popular due to their notable aesthetic appeal, efficiency of construction, adequacy for construction in weak soil, economically advantageous solution for moderate to large spans and uniqueness. Due to the current advances in analysis techniques by the use of computers there was enormous increase in the construction of such type of bridges. This expansion was significantly accompanied by technological developments like use of high strength material and advanced construction technique and which subsequently led to progressively larger and more slender bridges.

Thus Cable-stayed bridges have become the form of choice over the past several decades for bridges in the medium- to long-span range.

1.2 Necessity of Wind load analysis for Cable-stayed bridges

Cable-stayed bridges are subjected to variety of dynamic loads like traffic, wind, pedestrian and seismic loads which are very complex in nature. In addition to this the stay cables are very flexible structural elements generally characterized by small damping coefficients; it is understandable that these elements are prone to vibrations. As a result, they are susceptible to ambient excitations, which include those from seismic, wind and traffic loadings. In particular, since the geometric and structural properties of these bridges are complex as well as the characteristics of the excitations, the mechanisms underlying some of the vibrations still remain to be fully understood. The most important feature of this kind of structures is the high nonlinearities of geometry and material.

Many vibration phenomenons have been observed in cable supported bridges all over the world. Although the exact nature of the vibrations could not be predicted before 1980 as this phenomena were not well understood. The well-known collapse of Tacoma Narrows Bridge in 1940 clearly identified the importance of wind effects on long-span bridge performance. Extensive research has been carried out since then to better understand the effects of wind on long-span bridges, producing various analytical response prediction techniques. However, due to challenges related with full-scale measurements, these

prediction techniques have commonly been validated using only wind-tunnel experiments. Recent research has revolved around the conduct of long-term full-scale measurements on a cable-stayed bridge to compare actual bridge performance with those of analytical predictions.

1.3 Scope of Work:

The intent of this research is to present a detailed study of various phenomena's that induce vibrations in Cable-stayed bridges. The wind load analysis is carried out for a Cable-stayed bridge model for Indian terrain conditions. The wind load analysis is carried out on MIDAS CIVIL 2012 to check the behavior of bridge vulnerability against wind forces.

The scope of the present work is outlined as under:

- The main objective is to study the components of Cable-stayed bridges.
- To study the wind excitations phenomenon and the mechanisms of the wind induced vibrations and behavior of Cable-stayed bridges under wind loads.
- To determine the behavior of stay cables in Cable-stayed bridges. It involves the determination of natural frequency of stay cables and profile of the cable under axial tension and self weight of the cable.
- To model a Cable-stayed bridge for Indian terrain conditions in FEM software.
- Applying wind load on Cable-stayed Bridge model.
- Analysis of Cables-stayed Bridge for wind loads.
- To study the effect of wind loads on cables stays and deck under the wind loads.
- The study the overall effect of wind excitation on the bridge structure as a whole.
- To suggest mitigation measures for wind induced vibrations in Cable-stayed bridges.

1.4. Layout of the Dissertation

This report presents research work carried out towards objectives mentioned above. The entire report consists of six chapters. Each chapter deals with separate but inherently integrated tasks. The outline of the report is as follows:

Chapter 1 presents the necessity and the scope of the dissertation.

Chapter 2 is the detailed literature review of wind induced vibration and its effects on cables-stayed bridges. The state of the practice on wind excitations on bridges in structural engineering practice is reviewed.

Chapter 3 makes for better understanding of Cable-stayed bridges, its components. It also investigates the characteristics of wind loads on stays and bridge deck of cable-stayed bridge.

Chapter 4 presents the modeling methodology in software which includes consideration for modeling non-linearity in Cable-stayed bridge components especially the stay cables. This chapter will also describe the nature and magnitude of wind load application on Cable-stayed bridges.

Chapter 5 states the mitigation measures for wind induced vibrations in cable stayed bridges.

Chapter 6 states the conclusions of the research and recommendations on future research in the subject area.

Chapter 2

LITERATURE REVIEW

2.1. General

This chapter presents a review of relevant literature to bring out the background of the study undertaken in this dissertation. The research contributions which have a direct relevance are treated in greater detail. Some of the historical works which have contributed greatly to the understanding of the wind analysis of cable-stayed bridges are also described. First, a brief review of the historical background is presented. The concepts of structural aerodynamics, aerodynamics of bluff bodies, wind loading, and dynamic response of structures, related to work carried out in this thesis, are then discussed. The amount of the literature on the subject has increased rapidly in recent years; particularly to wind load application on cable-stayed bridges. Several of this is available in the proceedings of the conferences which are very helpful to understand the recent developments in wind engineering.

2.2. Historical Developments

In the past sixteen decades wind oscillations have severely damaged at least 11 major cable supported bridges. After the Tacoma Narrows Bridge disaster in 1940, lot of research has been carried out in the field of wind analysis of Cable Supported Bridges and on flow of fluids around structures, ranging from clarinet reeds to skyscrapers which caused destructive vibrations as well as useful vibrations. Extensive research has been carried out since then to better understand the effects of wind on long-span bridges, producing various analytical response prediction techniques. Also many phenomenass which caused vibrations were indentified but this research was mainly for the aircraft industry. Later these phenomena were put forward to the bridge engineering practice.

2.3. Analytical Work

Ahsan Kareem (2003) pays tribute to the "father of wind engineering," Jack E. Cermak, for his many valuable and pioneering contributions to the subject, followed by a reflection on the recent developments in wind effects on structures and an outlook for the

future. His work encompasses the following topics: modelling of wind field, structural aerodynamics, computational methods, dynamics of long -period structures, model to full-scale monitoring, codes/standards and design tools, damping and motion control devices.

B. N. Sun, Z. G. Wang, J. M. K and Y. Q. Ni proposed a nonlinear dynamic model for the simulation and analysis of a kind of parametrically excited vibration of stay cables caused by support motion in cable-stayed bridges. Based on this model, the oscillation mechanism and dynamic response characteristics of this kind of vibration are analyzed through numerical computation. They concluded that in cable-stayed bridges, if the ratio of natural frequencies of cable to bridge deck falls into certain range, serious parametric vibrations of the cables with large amplitude may occur. The cable dynamic response is dependent on the vibration level of the bridge deck, and the frequency and mass ratios of cable to deck, but independent of initial perturbation. The beating frequencies relate to tension force of the cable. The larger the static tension force is, the lower the beating frequency. The matching frequency exciting cable parametric vibration in deck motion also relates to the vibration amplitude of the deck and the mass ratio of cable to deck.

M. S. Pfei and R. C. Batista (1995) proposed a finite-element modal formulation to deal with cable stayed bridges under a laminar wind flow is presented and used to investigate their dynamic and stability behaviours. A comparison between results of the mode-by-mode method, in which all couplings are neglected, and the complete model, which includes many vibration modes, is presented. The dynamic responses obtained from the integration of the equations of motion, were used to investigate the dynamic behaviour of the chosen bridge examples, to evaluate critical wind velocities, and then to compare these velocities with those calculated through the mode-by-mode method. The results indicated that for wind velocities slightly greater than the critical velocity, these unstable dynamic responses can be strongly affected by the aerodynamic coupling, which occurs for the bridge with a not-too-bluff profile like that of the adopted box section. Finally, they proposed that a full appreciation of the aerodynamic coupling effect will still have to study for a. broader numerical and further experimental studies should be done.

Jin Cheng, Jian-Jing Jiang, Ru-Cheng Xiao, Hai-Fan Xiang investigated aerodynamic countermeasures using two-edge girder sections for a cable-stayed bridge. Wind tunnel tests were conducted to confirm the performance of the new countermeasures. Additional structural countermeasures based on increasing the rigidity of the bridge were also investigated. This study concluded that the addition of a horizontal member at the top of the

tower is the most effective method for increasing the flutter onset velocity. These aerodynamic countermeasures were also found to be economical.

Nicholas P. Jones and Robert H. Scanlan (2001) developed multimode flutter and buffeting analysis procedures. These procedures, which were based centrally on frequency domain methods, take into account the fully coupled aero elastic and aerodynamic response of long-span bridges to wind excitation. They reviewed the current state of the art in long-span bridge wind analysis, focusing the application of the theory to the stability (flutter) and serviceability (buffeting) analyses of a new long-span bridge in North America. This research work seeks to exhibit recent developments in the field to the interested structural/bridge engineer, outline alternative procedures available for assessment of wind effects on cable-supported bridges, and provide an overview of the basic steps in the process of a typical aerodynamic analysis and design.

Thai Huu-Tai and Kim Seung-Eock (2007) presented the theory and formulation of the nonlinear dynamic analysis of cable-stayed bridge. They have also proposed case studies of the behaviour of a cable-stayed bridge. They have developed computer software considering both geometric and material nonlinearities. The results of static behaviour, natural period as well as dynamic response of the cable-stayed bridge generated by SAP2000, ABAQUS, and proposed software are compared. The good results obtained in all cases of analysis prove that the proposed software can efficiently be used in predicting the nonlinear behaviour of cable-stayed bridges subjected to static and dynamic loading. The proposed software can efficiently be used in predicting the nonlinear behaviour of cable-stayed bridges subjected to static and dynamic loading.

Po Kwong Anthony Yiu (1982) presented the mathematical modelling of Cable-stayed bridges. He has proposed formulations of deformed geometry and element forces for the static and dynamic analysis of cable assisted bridges. He has also developed a static solution of cable assisted structures by dynamic relaxation. Also a review of the classical flutter theory and flutter of cable assisted bridges has been done.

S Katta (2009) has made a comparative study between various cable stayed bridges and its preliminary design considerations. Also the he has proposed modelling techniques in cable-stayed bridges. Also numerical modelling has been done and static non-linear analysis has been done under dead and live load. The general behaviour of Cable-stayed bridges has been discussed. The behaviour of stay cables in cable-stayed bridges i.e., cables profile under

axial tension and its own weight and natural frequencies of the inclined stay cables has been discussed.

ZHANG Xin-jun, SUN Bing-nan, XIANG Hai-fan (2004) worked on nonlinear multimode aerodynamic analysis of the Jingsha Bridge under erection over the Yangtze River, and the evolutions of structural dynamic characteristics and the aerodynamic stability with erection are numerically generated. Instead of the simplified method, nonlinear multimode aerodynamic analysis is suggested to predict the aerodynamic stability of cable-stayed bridges under erection. Their analysis showed that the aerodynamic stability maximizes at the relatively early stages, and decreases as the erection proceeds. The removal of the temporary piers in side spans and linking of the main girder to the anchor piers have important influence on the dynamic characteristics and aerodynamic stability of cable-stayed bridges under erection.

Younes. A. (1997) investigated the active damping of vibrations of the cable-stayed structures. He has developed a control law (Integral Force Feedback) which guarantees stability and damping, even for nonlinear systems. The efficiency and the robustness of this control law have been experimentally confirmed on several laboratory cable structure mock-ups; the structure is nicely damped, even at the parametric resonance. The control strategy has been implemented in a decentralized manner for cable structures with several cables. For demonstration purposes, a laboratory scale model has been designed with two dominant degrees of freedom (representing the torsion and the bending modes of the bridge deck) and provided with two cables equipped with active tendons. Experiments have been performed on this test article, and the properties of the Integral Force Feedback have been demonstrated. The torsion flutter of a cable-stayed bridge has been simulated on a laboratory mock-up using a specially designed control system involving a shaker and an accelerometer. It has been demonstrated that the flutter speed can be significantly increased when the decentralized active tendon is applied to the cable-stayed structure.

2.4. Experimental Work

Nicholas P. Jones and Ender Ozkan presented an example of the effects of wind on long-span bridges, producing various analytical response prediction techniques. However, due to challenges related with full-scale measurements, these prediction techniques have commonly been validated using only wind-tunnel experiments. They investigated long-term

efforts to monitor a cable-stayed bridge for a variety of purposes, including understanding the modal characteristics and wind-induced responses under ambient wind conditions. Using data files collected during various meteorological conditions, natural frequencies and mode shapes of the deck were found using an automated data analysis procedure. The measured modal frequencies, mode shapes, and RMS responses are observed to agree with the predicted values found from a finite element and aerodynamic analysis.

W. J. Wu, C. S. Cai and S. R. Chen (2004) experimentally studied cable vibration control with a MR damper. The performance of this damper was obtained experimentally with different loading frequencies and currents. A 7.16m-long stay cable with a prototype-to-model scale factor of eight is established for the vibration control study. Frequencies of the stay cable under different tension forces are measured and compared with those obtained through theoretical calculation. Then, by hanging a mass in the middle of the cable and by cutting the connecting rope, a free vibration control test is carried out and the acceleration time histories of the middle point and the 1/4th point of the cable are measured while the MR damper with different inside currents is installed at the 1/4th point. Also, a shaker is installed at 2.3% of the cable length close to the lower end to simulate a forced vibration control test. The measured data show that the damper is good for cable vibration control within its working current range (zero to maximum) though beyond some value, the control effect stays almost the same with increased current. It is also observed that the damper can reduce cable vibration under a variety of excitation frequencies, especially for the resonance cases.

J.A.Main and N.P.Jones made full-scale measurement programs that were designed to document the phenomenon over an extended period at full scale, and to assess the effectiveness of a proposed mechanical damper mitigation system. They identified three distinct regimes of cable vibration from the full-scale measurements: no-rain vibrations, moderate-rain vibrations, and heavy-rain vibrations. Also they discussed response characteristics of a few specific stays on one bridge; comparative studies have also been conducted to make conclusions of more general applicability. Finally, analytical models are being developed for prediction purposes and to provide guidance to designers who desire to eliminate the problem of excessive stay-cable vibration.

Roman Geier and Rainer Flesch has done an overview concerning the experiences derived from ambient vibration monitoring of stay cables. They proposed a state of art monitoring approach for vibrations in cable-stayed bridges. They also have made investigations on damping trend of stay cables.

Chapter 3

THEORY OF CABLE-STAYED BRIDGES

3.1. Introduction to Cable Stayed Bridge

A cable-stayed bridge is a bridge that consists of one or more columns (normally referred to as *towers* or *pylons*), with cables supporting the bridge deck. Cable-stayed bridges are constructed along a structural system that comprises an orthotropic deck and continuous girders, which are supported by stays, that is, inclined cables passing over or attached to towers or pylons located at the main piers.

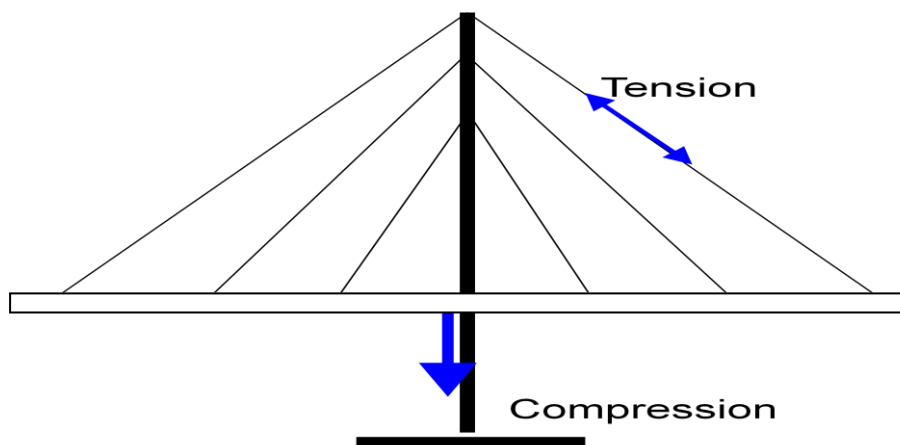


Figure 3.1. Behaviour of Cable-stayed Bridge.

Modern cable-stayed bridges present a three-dimensional system consisting of stiffening girders, transverse and longitudinal bracings, orthotropic type deck and supporting parts such as towers (or pylons) in compression and inclined cables in tension. Therefore, we can say for the vast majority of all cable-stayed bridges the structural system can be divided into main components as follows: -

- 1) The Stiffening girder (or truss) with the bridge deck,
- 2) The Cable system supporting the stiffening girder,
- 3) The Towers (or pylons) supporting the cable system,
- 4) The Anchor blocks (or the anchor piers) supporting the cable system vertically or horizontally.

The cables are connected directly to the deck and induce significant axial forces into the deck. The structure is consequently self-anchoring and depends less on the foundation

conditions. The cables and the deck are erected at the same time, which speeds up the construction time and reduces the amount of temporary works required.

3.2.1. Arrangement of the stay cables

According to the various longitudinal cable arrangements, cable-stayed bridges could be divided into the following four systems:

a) Radial or Converging System

In this type of system all cables are connected to the top of the tower. Structurally, this system can be said as the best among all, as by taking all the cables to the tower top the maximum inclination to the horizontal is achieved and consequently amount of steel for the cables is minimized. However, at the top the tower the cable supports or saddles within the tower may become very congested and also a considerable amount of vertical force is to be transferred. Thus the detailing of the structure becomes quite complex.

b) Harp or Parallel System

In this type of the system the cables are connected to the tower at different heights, and also placed parallel to each other. This type of system cause bending moments in the structure also it is necessary to study whether the support of the lower cables can be fixed at the tower legs or must be made in a horizontal direction. The harp-shaped give an excellent strength for the main span, if each cable is anchored to a pier on the riverbanks for example in the Knie Bridge at Dusseldorf, Germany. The quantity of the steel required for a harp-shaped cable arrangement is slightly higher than for a fan-shaped arrangement, thus if we choose a higher tower (or pylon) it will increase the stiffness of the cable system against deflections.

c) Fan or Intermediate System

This system represents a combination of the radiating and harp system. The cables emanate from the top of the tower with equal spacing and connect with equal spacing along the superstructure. As the spaces are small near the top of the tower the cables are not parallel and the forces remain small so that single ropes can be used and all the ropes have fixed connections in the tower. The Nord Bridge, Bonn, Germany is a typical example of this kind of arrangement.

d) Star System

The star system is an aesthetically attractive cable arrangement. However, it contradicts the principle that the points of attachments of the cables should be distributed as much as possible along the girder.















Single	Double	Triple	Multiple	Combined	
					Radiating
					Harp
					Fan
					Star

Figure 3.2. Arrangement of Stay Cables.

3.2.2. Selection of Cable Configuration

The selection of cable configuration and number of cables is dependent mainly on length of the span, type of loadings, number of roadway lanes, height of towers, and the designer's individual sense of proportion and aesthetics. Cost factors also have a great influence on the selection of the cable arrangements, as using less number of cables results large cable forces, which requires massive and complicated anchorage systems connecting to the tower and superstructure. These connections become sources of heavy concentrated loads requiring additional reinforcement of webs, flanges, and stiffeners to transfer the loads to the bridge girders and distribute them uniformly throughout the structural system. A large number of cables distribute the forces more uniformly throughout the deck structure without major reinforcement, which provides continuous support thus, permitting the use of shallow depth girder that also tends to increase the stability of the bridge against dynamic wind forces. In case of radiating cable arrangement as the cable stays are at the maximum angle of

inclination to the bridge girders, the cables are in an optimum position to support the gravity dead and live loads and simultaneously produce minimum axial component acting on the girder system. On the other hand as this system have all the cables at the top, thus concentrating the entire load on the tower which produces large shear and moments in the tower and also presenting difficulties in anchoring all the cables at the top or over the saddle, thus complicating the transfer of the vertical force.

3.2.3. Positions of the cables in space

There are two basic arrangements out of the many planes in which the cable stays are disposed which are: two-plane and single-plane systems. Among which the two-plane systems can be further divided in two types as follows:

3.2.3.1. The Two Planes System

a) Two Vertical Planes System

In this type of system there are two parallel sets of cables and the tower on the either sides of the bridge, which lie in the same vertical plane. Here two alternative layouts may be adopted when using this system:

- i) The cable anchorages may be situated outside the deck structure, which is better than the other in terms of space as no deck area of the deck surface is obstructed by the presence of the cables and the towers. There is however, a disadvantage in that the transverse distance of the cable anchorage points from the webs of the main girders requires substantial cantilevers to be constructed in order to transfer the shear and the bending moment into the deck structure. Also the substructure, especially the piers for the towers have to be longer, because in this case the towers stand apart and outside the cross-section of the bridge.
- ii) When the cables and tower lie within the cross-section of the bridge, the area taken up cannot be utilized as a part of the roadway and may be only partly used for the sidewalk. Thus as area of the deck surface is made non-effective and has to be compensated for by increasing overall width of the deck.

b) Two Inclined Planes System

In this system the cables run from the edges of the bridge deck to a point above the centreline of the bridge on an A-shaped tower or λ -shaped or diamond shaped pylon. This arrangement can be recommended for very long spans where the tower has to be very high and needs the lateral stiffness given by the triangle and the frame junction. Joining all cables on the top of tower has a favourable effect regarding

3.2.3.2. The Single Plane System

This type of system consists of bridges with only one vertical plane of stay cables along the middle longitudinal axis of the superstructure and as the cables are located in a single centre vertical strip thus all the space is utilized by the traffic. This arrangement requires a hollow box main girder with considerable tensional rigidity in order to keep the change of cross-section deformation due to eccentric live load within allowable limits. This system also creates a lane separation as a natural continuation of the highway approaches to the bridge. It should be noticed that all the possible variations regarding the longitudinal arrangements of the cables used with two planes bridges are also applied to single centre girder bridges. This is an economical and aesthetically acceptable solution, providing an unobstructed view from the bridge; it also offers advantage of relatively small piers as their size is determined by the width of main girder. A possible disadvantage of this system is the fact that maximum cable load is transferred to the main superstructure girder, thereby requiring additional reinforcement and stiffening of the deck. Web plates and bottom flange would be also required in order to distribute the load uniformly throughout the cross-section of the superstructure members.

3.2.4. Tower (or Pylon) Types

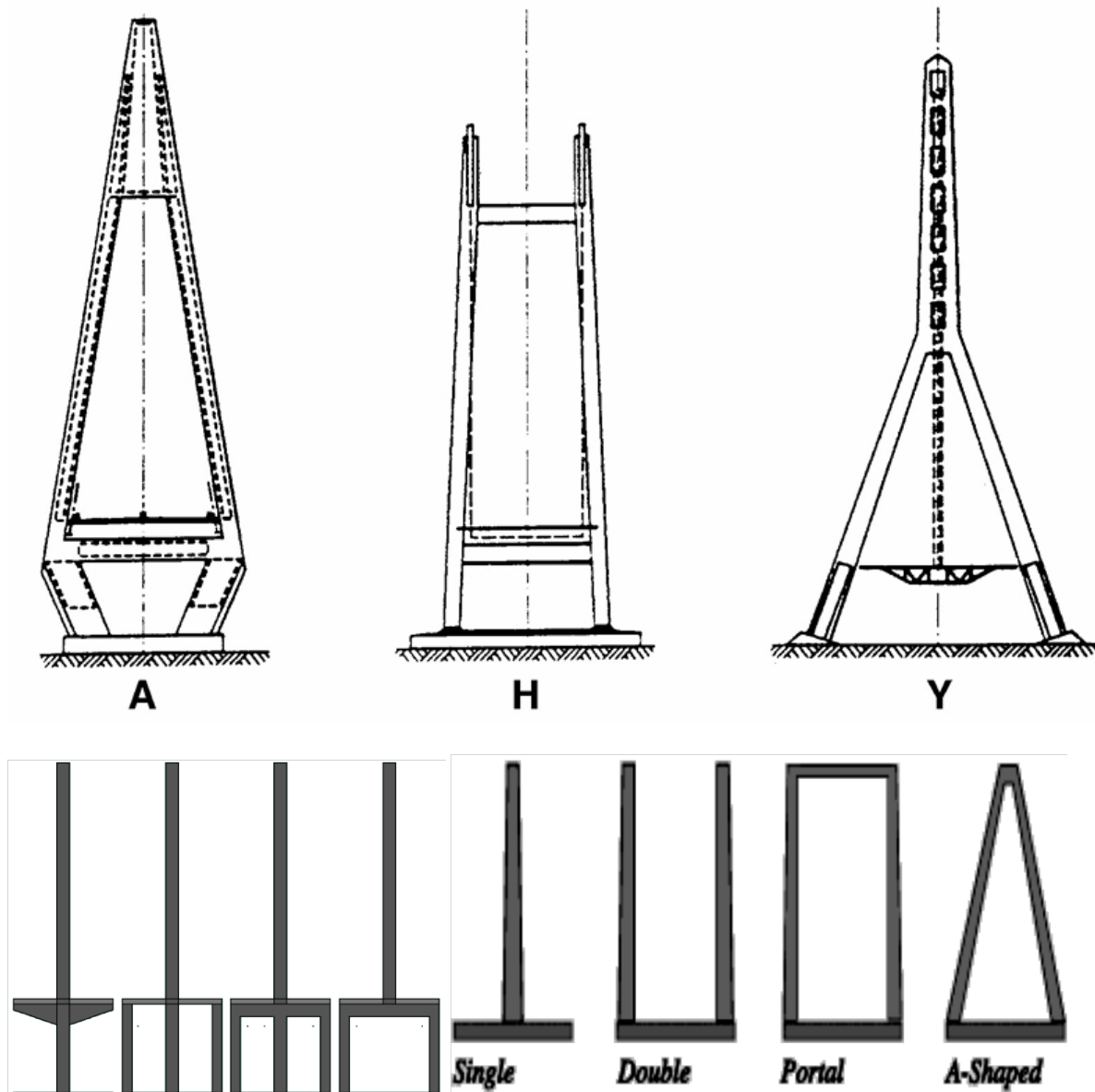


Figure 3.3. Various basic tower shapes.

The various basic tower shapes are illustrated in above figures. There are many modifications to these shapes, each with its own advantages, disadvantages and aesthetic appeal. Towers can be of steel, concrete or a composite. In the composite type, the inner shell can be of steel with an outer shell of concrete for aesthetic purposes or a steel cable anchoring system composite with the concrete shell. Most towers have hollow columns that accommodate ladders, hoists and power feeds. Investigations of cable-stayed bridges indicated that the horizontal forces of the cables were relatively small, so that freely standing

tower legs could be used without disadvantage. The inclined cables even give a stabilizing restraint force when the top of the tower is moved transversely. With single tower or twin towers with no cross-member, the tower is stable in lateral direction as long as the level of the cable anchorages is situated above the level of the base of the tower. In case of displacement of the top of the tower due to wind forces, the length of the cable increases resulting increase in tension, which provides a restoring force. Longitudinal movement of the tower is restricted by the restraining effect of the cables fixed at the saddles or tower anchorages.

The towers can have three different kinds of supports as follows:

- a) **Towers Fixed at foundation** Towers with fixed legs are relatively flexible, and loading and temperature do not cause significant stress in the structure. However, large bending moments are produced in tower in this case. The main girders pass between the frame legs and are supported on the transverse beam.
- b) **Towers Fixed at Superstructure** In case of the single-box main –bridge system, the towers are generally fixed to the box. With arrangement it is necessary not only to reinforce the box but also to provide strong bearings. The supports also may resist the additional horizontal forces caused by the increased friction forces in the bearings.
- c) **Hinged Towers** For structural reasons, the towers may be hinged at the base in the longitudinal direction of the bridge. This arrangement reduces the bending moments in the towers and the number of redundant, which simplifies analysis of the overall structure. Also, in case with bad soil conditions, linear hinges at the tower supports are provided, allowing longitudinal rotation, so that bending moments are not carried by the foundation.

3.2.5. Deck Types

Most cable-stayed bridges have orthotropic decks that differ from another only as far as the cross-sections of the longitudinal ribs and spacing of the cross-girders is concerned. The orthotropic deck performs as the top chord of the main girders or trusses. It may be considered as one of the main structural elements that lead to the successful development of the modern cable-stayed bridges.

3.2.6. Main Girder

In cable stayed bridges, the girder is designed to sustain bending, torsion and the axial force component induced by the cables. Stiffening truss and solid web girders are the two types of girders used most frequently in cable-stayed bridges. The disadvantages of using stiffening truss are:

- It requires more fabrication.
- Most difficult to maintain.
- More susceptible to corrosion.
- Somewhat unappealing.
- Poor aerodynamic characteristics.

Solid web girders for various types of bridge deck cross sections are:

- Plate Girders.
- Box Girders.

The disadvantage of using plate girder is, it has low value of torsional rigidity. The box girders may be of rectangle or trapezoidal in shape. In the design of decks, the maximum preference is to use the orthotropic box girder arrangement with the trapezoidal configuration, since it is having good aerodynamic stability. In single plane system the cables assist the bridge deck in bending, hence torsion has to be resisted by the stiffening girder alone. Torsionally stiff single box girders and multiple web box girders provide the best solution in this case. With double plane and inclined plane arrangements, the cables restrain both bending and torsion and thus trusses and plate girders can be used as stiffening girders.

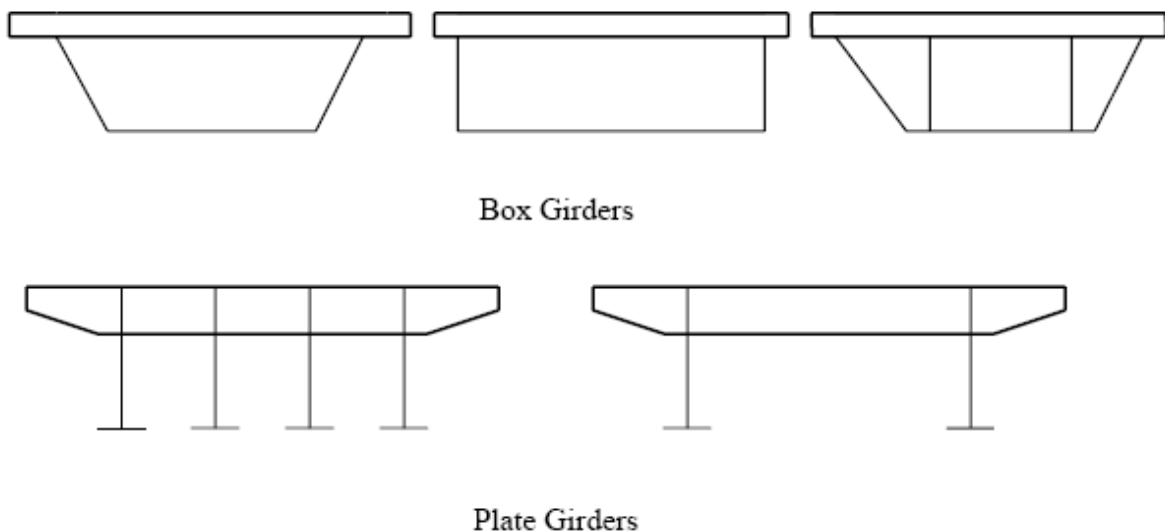


Figure 3.4. Shapes of Girders.

3.2.6 Cable Types

A cable may be composed of one or more structural ropes, structural strands, locked coil strands or parallel wire strands. A strand is an assembly of wires formed helically around centre wire in one or more symmetrical layers. A strand can be used either as an individual load-carrying member, where radius or curvature is not a major requirement, or as a component in the manufacture of the structural rope. A rope is composed of a plurality of strands helically laid around a core. In contrast to the strand, a rope provides increased curvature capability and is used where curvature of the cable becomes an important consideration.

There are three types of strand configuration:

- 1) Helically-wound strand
- 2) Parallel wire strand
- 3) Locked Coil strand

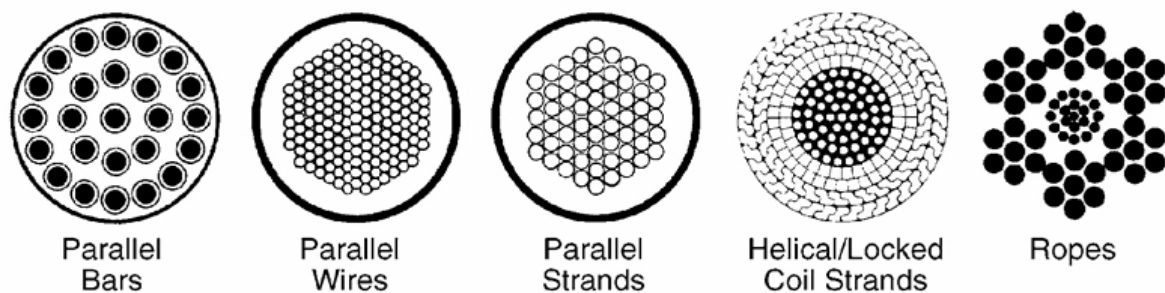


Figure 3.5. Various cable patterns.

3.3. Wind loading in stay cables

Wind is one of the most important factor in the design of cable stayed bridges, particularly of stay cables. These structural elements suffer both from direct excitation along the surface and from indirect action on the deck and towers, which result in oscillation at supports.

The study of wind effects is normally conducted by separating the static component, associated with a mean flow velocity of air, and dynamic component, related with vortex shedding and atmospheric turbulence. The report presents a brief description of wind loads applied to stay cables, concentrating on the effects of the corresponding dynamic component. Particular vibrating phenomenon are introduced, namely buffeting, vortex-shedding, galloping, aerodynamic interference, rain-wind induced vibration and a set of vibration phenomena that has been identified recently, like dry galloping and drag crisis phenomena. The probable mechanisms that govern these phenomena are explained according to various theories.

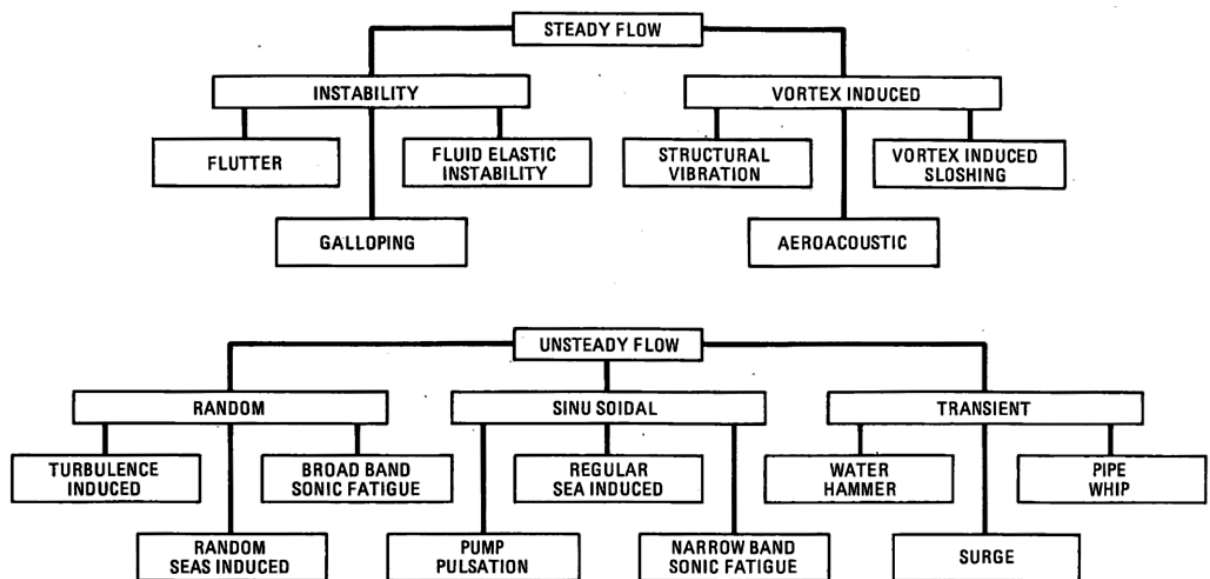


Figure 3.6. A classification of flow-induced vibrations.

3.4.1. General

When related to structural engineering problems, the wind is a flow generally characterized by three time-dependent velocity components $U(t)$, $V(t)$, and $W(t)$, along three mutually perpendicular directions. These components depend on mean velocity U , which is horizontal and has dominant wind direction, and on the fluctuating component $u(t)$, $v(t)$ and $w(t)$, according to

$$U(t) = U + u(t) \quad \dots\dots\dots(3.1a)$$

$$V(t) = v(t) \quad \dots\dots\dots(3.1b)$$

$$W(t) = w(t) \quad \dots\dots\dots(3.1c)$$

By immersing the body (a stay cable) in this flow, surface pressures are generated. If the body is fixed, the developed pressures depend on the characteristics of the flow and on geometry of the body. If the body is free to oscillate, the developed pressures are modified by vibrations. This usually happens in the case of stay cables.

Although in practice these effects are related, they are frequently analyzed separately for the sake of simplicity.

Considering the stay cable represented by a non-circular cylinder of infinite length immersed in a two-dimensional flow, the incident forces per unit length are calculated from integration of the generated surface pressures under the following conditions:

- a. Fixed cylinder immersed in a smooth flow.
- b. Fixed cylinder immersed in turbulent flow.
- c. Moving cylinder immersed in a turbulent flow.

These independent conditions allow the identification and discussion of particular features of the flow around the body, like shape coefficients and their variation with Reynolds number (R_e), the formation of vortices in the wake of the flow and the development of aerodynamic damping.

a. Fixed cylinder immersed in smooth flow

The resultant wind loads on structure are expressed in a Cartesian reference system (O, d, l), whose axis d is obtained by a rotation axis x from a general reference system (O, x, y) by an angle β counter-clockwise, in order to align with the wind velocity vector U (Fig.3.7. (a))

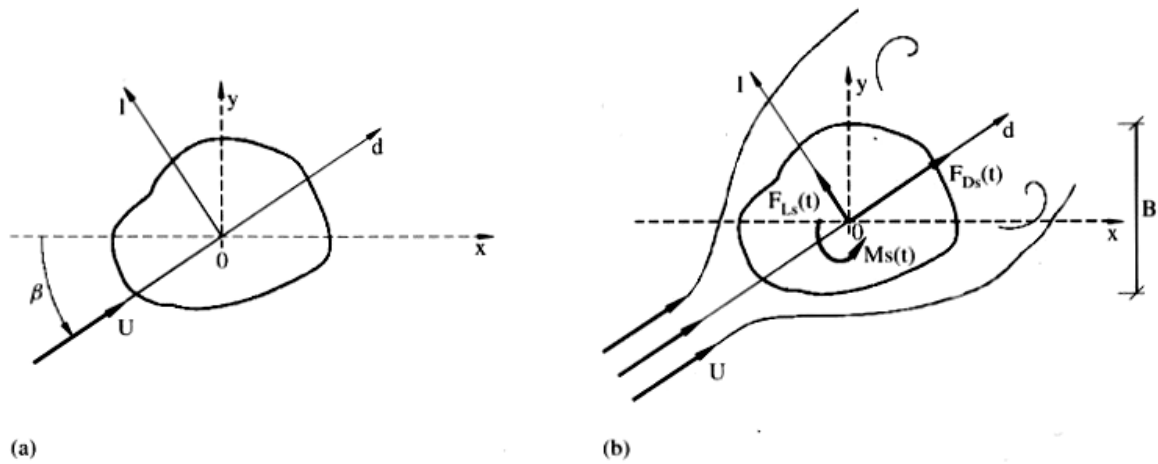


Figure 3.7. – Fixed rigid cylinder of infinite length immersed in a smooth flow: (a) Reference Cartesian systems and wind velocity field; (b) aerodynamic forces.

According to the representation in (Fig.3.7.(b)), two force components $F_{Ds}(t)$ and $F_{Ls}(t)$ in the along-flow direction occur, designated as drag and lift forces, as well as a moment $M_s(t)$ acting on the elastic centre of the Body O, which are defined by

$$F_{Ds}(t) = F_D + f_{Ds}(t) \dots\dots\dots(3.2a)$$

$$F_{Ls}(t) = F_L + f_{Ls}(t) \dots\dots\dots(3.2b)$$

$$M_s(t) = M + m_s(t) \dots\dots\dots(3.2c)$$

Where F_D , F_L and M represent the mean values of wind forces, and $f_{Ds}(t)$, $f_{Ls}(t)$ and $m_s(t)$ are nil mean fluctuations. The values of these components are determined from the balance between inertial and viscous forces around the cylinder that is quantified through Reynolds number Re , defined as

$$Re = \frac{UB}{\nu} \dots\dots\dots(3.3)$$

Where B is a representative dimension of cylinder, U is the uniform wind velocity and ν is the kinematic viscosity of air.

By increasing the flow velocity, the Reynolds number increases. At $Re \approx 20$ the flow separates creating two symmetrical vortices near the downstream surface of the cylinder (Fig.3.8. (b)). At an increased Reynolds number of 30, the symmetrical vortices are broken and replaced by cyclic alternating vortices that form by turn at the top and bottom surfaces

and are swept away downstream to form a vortex trail, designated as the Von Karman vortex trail (Fig.3.8. (c)).

As the Reynolds number increases into range of $5000 \leq R_e \leq 200000$, the attached flow upstream of the separation point remains laminar, while transition to turbulent flow occurs in the wake (Fig.3.8. (d)), further downstream from the cylinder for the smaller R_e number, and closer to the cylinder surface for the higher R_e . Finally, for a very large R_e number, i.e. $R_e \geq 200000$, the wake narrows, meaning that reduced forces are acting on the cable (Fig 3.8. (e)).

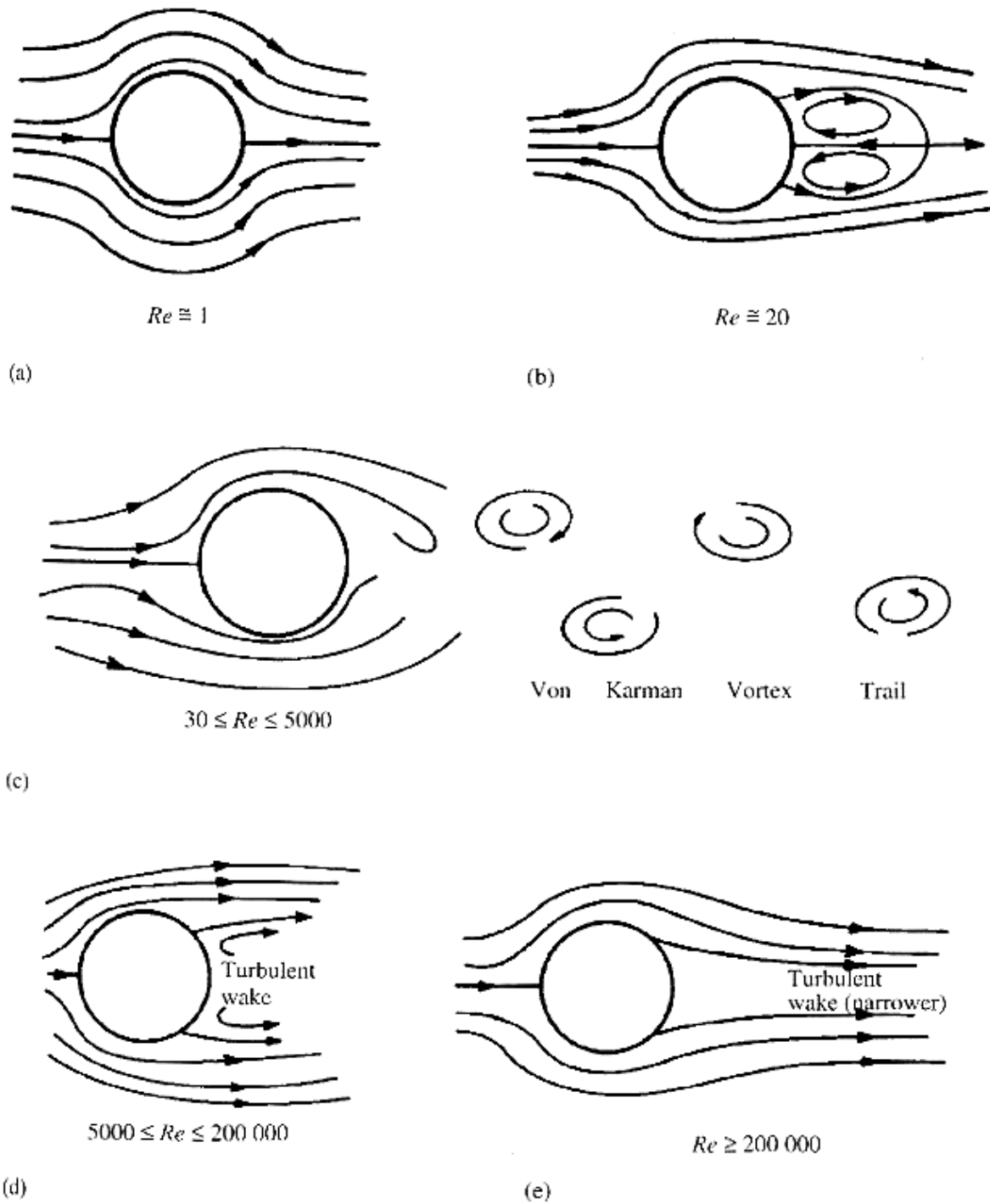


Figure-3.8. Flow past circular cylinder.

(Fig.3.8.), Illustrates the organization of the flow with increasing Reynolds number for particular case of cylinder of diameter D ($R=D$)

The mean wind forces F_D , F_L and M , representing the static component of wind loads, are generally decided as

$$F_D = \frac{1}{2} \rho U^2 B C_D(\beta) \dots\dots\dots(3.4a)$$

$$F_L = \frac{1}{2} \rho U^2 B C_L(\beta) \dots\dots\dots(3.4b)$$

$$M = \frac{1}{2} \rho U^2 B C_M(\beta) \dots\dots\dots(3.4c)$$

Where ρ the density of air, B is the representative dimension of the body (Fig 3.7. (b)) that coincides with the outer diameter D for a circular cylinder, and $C_D(\beta)$, $C_L(\beta)$ and $C_M(\beta)$ are shape coefficients, drag life and moment coefficients, respectively, whose values depend on the characteristics of the cylinder surface and on the Reynolds number.

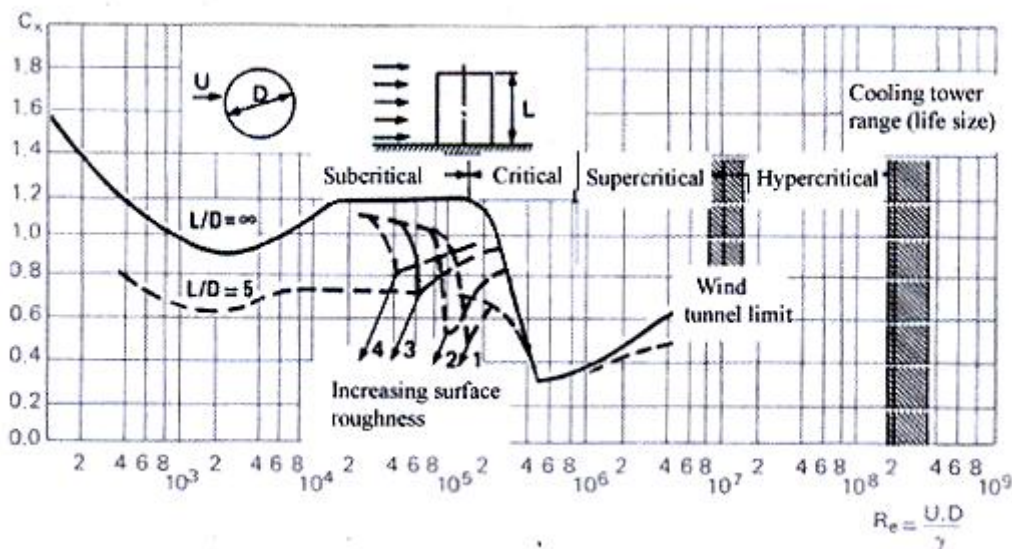


Figure- 3.9. Variation of CD with Re for a circular cylinder

(Fig.3.9.) illustrates the variation of C_D with Re for a circular cylinder with varying surface roughness, obtained from wind tunnel tests.

Considering the stay cable diameter in the range of 0.1-0.3m and the mean velocity of interest in the range of 5-50 m/s, the Reynolds number is in the range of $3 \times 10^4 - 10^6$. The analysis of (Fig.3.9.) shows three regions are defined for that range of Re value: the subcritical region is associated with low Re numbers and relatively constant C_D values of around 1.2; the critical region defined for Re values in the range of $2 \times 10^5 - 8 \times 10^5$, depending on the roughness of the surface, in which C_D can drop to around 0.4, corresponds to the transition from laminar to turbulent flow; and the supercritical region for which C_D increases slightly.

It is considered that for extreme wind speeds stay cables are normally in the supercritical region and a value of C_D of 0.7 is used for circular cross-sections. It should be noted that non-circular cross-sections have very different drag and lift coefficients. For stranded cables, average value of C_D of 1.2 is found. Considering that the wind load on the stay cables can be close or even more than 50% of the total transverse loads on bridge structure, the choice of cable cross-section becomes a matter of utmost importance.

The fluctuating components of wind loads $f_{Ds}(t)$, $f_{Ls}(t)$ and $m_s(t)$ in the expression (3.2) are primarily associated with the vortex shedding that occurs in the wake of the cylinder and can be approximated by

$$f_{Ds}(t) = \frac{1}{2} \rho U^2 B c_{Ds} \sin(4\pi f_v t) \dots\dots\dots (3.5a)$$

$$f_{Ls}(t) = \frac{1}{2} \rho U^2 B c_{Ls} \sin(4\pi f_v t) \dots\dots\dots (3.5b)$$

$$m_s(t) = \frac{1}{2} \rho U^2 B c_{Ms} \sin(4\pi f_v t) \dots\dots\dots (3.6c)$$

Where c_{Ds} , c_{Ls} and c_{Ms} are non-dimensional wake coefficients and f_v is the shedding frequency of the vortices, defined as a function of the Strouhal number St

$$f_v = \frac{U St}{B} \dots\dots\dots (3.6)$$

The Strouhal number St depends upon the shape of the cross section and is approximately constant with the Reynolds number for a wide range of Re , as shown in (Fig.3.9.) that presents the measurement on circular cylinders for different values of the roughness k/D .

For practical applications with circular cylinders, a constant value of St of 0.2 can be considered.

3.4.1.2. Fixed cylinder immersed in turbulent flow

Consider the fixed cylinder is immersed in a turbulent flow that is characterized by the same dominant direction and mean velocity U , and by the fluctuations $u(t)$ and $v(t)$ in the along-wind and across-wind directions respectively. (Fig 3.10.a.)

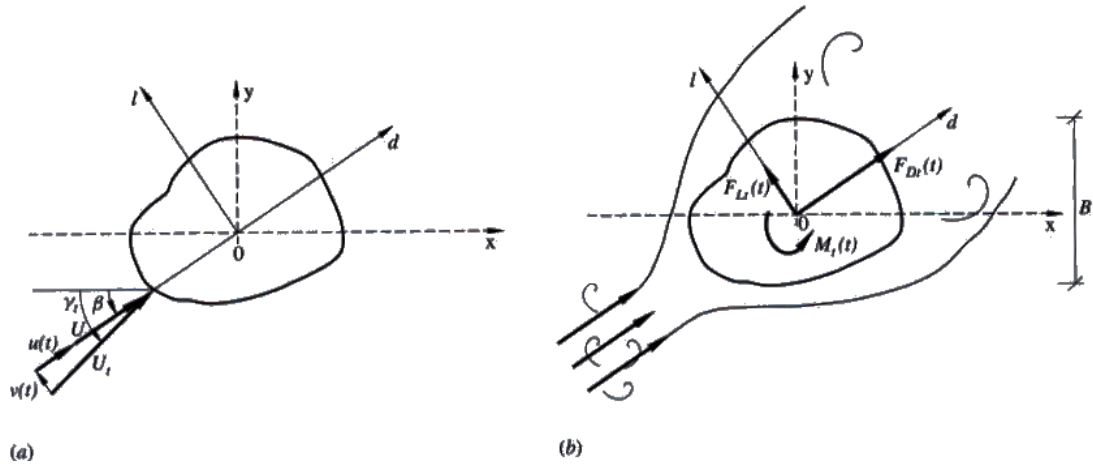


Figure-3.10. Fixed cylinder of Infinite length immersed in turbulent flow: (a) Reference Cartesian system and wind velocity field; (b) aerodynamic forces.

Assuming a small turbulence ($u/U \ll 1$; $v/U \ll 1$), the drag and lift forces and the moments over the cylinder in the turbulent flow, $F_{Dt}(t)$, $F_{Lt}(t)$ and $M_t(t)$, can be respectively obtained from a linearised approximation involving following components,

$$F_{Dt}(t) = F_{Dt} + f_{Du}(t) + f_{Dv}(t) + f_{Dw}(t) \quad \dots\dots\dots (3.7a)$$

$$F_{Lt}(t) = F_{Lt} + f_{Lu}(t) + f_{Lv}(t) + f_{Lw}(t) \quad \dots\dots\dots (3.7b)$$

$$M_t(t) = M_t + m_u(t) + m_v(t) + m_w(t) \quad \dots\dots\dots (3.7c)$$

In these expressions, F_{Dt} , F_{Lt} and M_t represent the mean wind drag, lift and moment components of load in the turbulent flow, given as function of the corresponding shape coefficients $C_{Dt}(\beta)$, $C_{Lt}(\beta)$, and $C_{Mt}(\beta)$ as

$$F_{Dt} = \frac{1}{2} \rho U^2 B C_{Dt}(\beta) \quad \dots\dots\dots (3.8a)$$

$$F_{Lt} = \frac{1}{2} \rho U^2 B C_{Lt}(\beta) \quad \dots\dots\dots (3.8b)$$

$$M_t(t) = \frac{1}{2} \rho U^2 B C_{Mt}(\beta) \quad \dots\dots\dots (3.8c)$$

It should be noted that turbulence tends to lead to a decrease of the shape coefficient.

The terms $f_{Du}(t)$, $f_{Lu}(t)$ and $m_u(t)$ in the expression (3.7.) represent the forces induced by the turbulence component u , while the terms $f_{Dv}(t)$, $f_{Lv}(t)$ and $m_v(t)$ represent the forces induced by the turbulence component v . These forces are expressed as function of the shape coefficients $C_{Dt}(\beta)$, $C_{Lt}(\beta)$ and $C_{Mt}(\beta)$ and of the corresponding derivatives with respect to the angle γ_t ,

$$f_{Du}(t) = \rho U u(t) B C_{Dt}(\beta) \dots\dots\dots (3.9a)$$

$$f_{Lu}(t) = \rho U u(t) B C_{Lt}(\beta) \dots\dots\dots (3.9b)$$

$$M_u(t) = \rho U u(t) B^2 C_{Mt}(\beta) \dots\dots\dots (3.9c)$$

and

$$f_{Dv}(t) = \frac{1}{2} \rho U v(t) B (C'_{Dt}(\beta) - C_{Lt}(\beta)) \dots\dots\dots (3.10a)$$

$$f_{Lv}(t) = \frac{1}{2} \rho U v(t) B (C_{Dt}(\beta) + C'_{Lt}(\beta)) \dots\dots\dots (3.10b)$$

$$m_v(t) = \frac{1}{2} \rho U v(t) B^2 C'_{Mt}(\beta) \dots\dots\dots (3.10c)$$

The last terms of expressions, $f_{Dw}(t)$, $f_{Lw}(t)$ and $m_w(t)$, represent the forces produced by the vortex wake. The harmonic nature of these forces in the uniform flow is disturbed by the presence of turbulence, leading to the following approximation,

$$f_{Dw}(t) = \frac{1}{2} \rho U^2 B c_{Dw}(t) \dots\dots\dots (3.11a)$$

$$f_{Lw}(t) = \frac{1}{2} \rho U^2 B c_{Lw}(t) \dots\dots\dots (3.11b)$$

$$m_w(t) = \frac{1}{2} \rho U^2 B c_{Mw}(t) \dots\dots\dots (3.11c)$$

And $c_{Dw}(t)$, $c_{Lw}(t)$ and $c_{Mw}(t)$ are the equivalent drag, lift and moment coefficients, respectively, measured in the wake of the cylinder.

3.4.1.3. Moving cylinder immersed in turbulent flow

Consider a cylinder immersed in a turbulent flow. Assuming that due to the flexibility of the cylinder, two translator and one rotation components, $d(t)$, $l(t)$ and $\theta(t)$ are possible, as represented in the (Fig.3.11.)

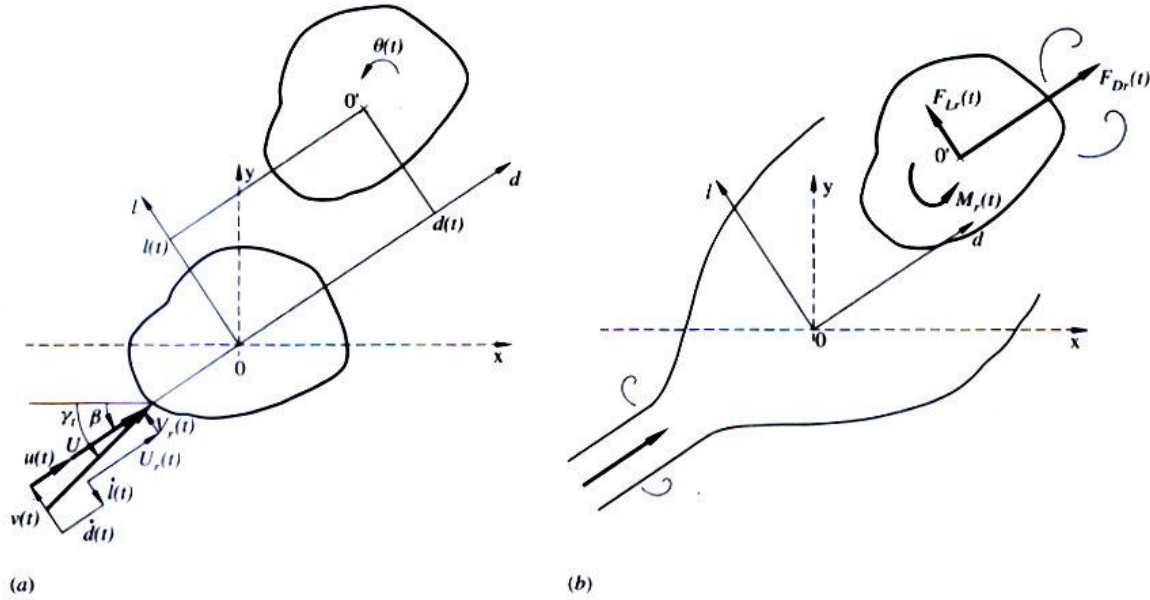


Figure- 3.11. Moving cylinder of Infinite length immersed in turbulent flow: (a) Reference Cartesian system and wind velocity field; (b) aerodynamic forces.

Owing to the motion of the cylinder, a relative velocity can be defined, whose along-wind and across-wind components, $U_r(t)$ and $V_r(t)$, respectively are

$$U_r(t) = U + u(t) - \dot{d}(t) \quad \dots\dots\dots (3.12a)$$

$$V_r(t) = v(t) - \dot{l}(t) \quad \dots\dots\dots (3.12b)$$

The symbol “.” in the equation (3.12) represents derivative with respect to time.

Considering small displacements and turbulence and assuming quasi-stationarity, the linearised resultant forces actuating the cylinder, $F_{Dr}(t)$, $F_{Lr}(t)$ and $M_r(t)$ can then be approximated by,

$$F_{Dr}(t) = F_{Dt} + f_{Du}(t) + f_{Dv}(t) + f_{Dw}(t) + f_{Dq}(t) + f_{D\dot{q}}(t) \quad \dots\dots\dots (3.13a)$$

$$F_{Lr}(t) = F_{Lt} + f_{Lu}(t) + f_{Lv}(t) + f_{Lw}(t) + f_{Lq}(t) + f_{L\dot{q}}(t) \quad \dots\dots\dots (3.13b)$$

$$M_r(t) = M_t + m_u(t) + m_v(t) + m_w(t) + m_{\theta q}(t) + m_{\theta\dot{q}}(t) \quad \dots\dots\dots (3.13c)$$

The first four terms in the second members of these expressions are defined above (expression no to no), representing by order the mean wind forces and the fluctuations due to along-wind and across-wind turbulence, and to wake effects. The last two terms in expression no are the fluctuations of the forces generated by the displacements and velocity of the cylinder, the so-called self excited or aero-elastic forces, and are defined according to

$$f_{Dq}(t) = -\frac{1}{2}\rho U^2 \theta(t) B C'_{Dt}(\beta) \dots\dots\dots (3.14a)$$

$$f_{Lq}(t) = -\frac{1}{2}\rho U^2 \theta(t) B C'_{Lt}(\beta) \dots\dots\dots (3.14b)$$

$$m_{\theta q}(t) = -\frac{1}{2}\rho U^2 \theta(t) B C'_{Mt}(\beta) \dots\dots\dots (3.14c)$$

$$f_{i\dot{q}}(t) = -\rho U \dot{d}(t) B C_{Dt}(\beta) - \frac{1}{2}\rho U \dot{i}(t) B (C'_{Dt}(\beta) - C_{Lt}(\beta)) \dots\dots\dots (3.15a)$$

$$f_{D\dot{q}}(t) = -\rho U \dot{d}(t) B C_{Lt}(\beta) - \frac{1}{2}\rho U \dot{i}(t) B (C_{Lt}(\beta) + C'_{Lt}(\beta)) \dots\dots\dots (3.15b)$$

$$m_{\theta\dot{q}}(t) = -\rho U \dot{d}(t) B^2 C_{Mt}(\beta) - \frac{1}{2}\rho U \dot{i}(t) B^2 C'_{Mt}(\beta) \dots\dots\dots (3.15c)$$

3.4.1.4. Linearised equation of motion

The motion of the cylinder when actuated by a turbulent wind flow can be described by the following linearised system of equations,

$$\underline{M}\ddot{\underline{q}}(t) + \underline{C}\dot{\underline{q}}(t) + \underline{K}\underline{q}(t) = \underline{F}_r(t) \tag{3.16}$$

Where $\ddot{\underline{q}}(t)$, $\dot{\underline{q}}(t)$ and $\underline{q}(t)$ are the acceleration, velocity and displacement vectors of the cylinder, whose components are

$$\ddot{\underline{q}}(t) = \begin{bmatrix} \ddot{d}(t) \\ \ddot{\theta}(t) \\ \ddot{l}(t) \end{bmatrix}; \quad \dot{\underline{q}}(t) = \begin{bmatrix} \dot{d}(t) \\ \dot{\theta}(t) \\ \dot{l}(t) \end{bmatrix}; \quad \underline{q}(t) = \begin{bmatrix} q(t) \\ \theta(t) \\ l(t) \end{bmatrix} \tag{3.17}$$

The matrices \underline{M} , \underline{C} and \underline{K} represent the cylinder (cable) mass, viscosity damping and stiffness per unit length with respect to $\underline{q}(t)$, and the vector forces $\underline{F}_r(t)$ represent the wind load, whose components are grouped as

$$\underline{F}_r(t) = \begin{bmatrix} F_{Dr}(t) \\ F_{Lr}(t) \\ M_r(t) \end{bmatrix} \tag{3.18}$$

Separating $\underline{F}_r(t)$ in two components, one associated with mean, turbulent and wake effects, $\underline{F}(t)$, and the other with the aero-elastic effects, $\underline{F}_a(t)$ yields

$$\underline{F}_r(t) = \underline{F}(t) + \underline{F}_a(t) \tag{3.19}$$

With

$$\underline{F}(t) = \begin{bmatrix} F_{Dt} + f_{Du}(t) + f_{Dv}(t) + f_{Dw}(t) \\ F_{Lt} + f_{Lu}(t) + f_{Lv}(t) + f_{Lw}(t) \\ M_t + m_u(t) + m_v(t) + m_w(t) \end{bmatrix}; \quad \underline{F}_a(t) = \begin{bmatrix} f_{Dq}(t) + f_{D\dot{q}}(t) \\ f_{Lq}(t) + f_{L\dot{q}}(t) \\ m_{\theta q}(t) + m_{\theta\dot{q}}(t) \end{bmatrix} \tag{3.20}$$

The dependence of the aero-elastic forces on cylinder's displacements and velocities allows the expression of these force components as

$$\underline{F}_a(t) = -\underline{C}_a\dot{\underline{q}}(t) - \underline{K}_a\underline{q}(t) \tag{3.21}$$

Where the matrices \underline{C}_a and \underline{K}_a can be understood as an aerodynamic viscous damping and an aero-elastic stiffness matrix, and are given, whenever small disturbance turbulence are assumed, according to the expression no and no, as

$$\underline{C}_a = \frac{1}{2} \rho U B \begin{bmatrix} 2C_{Dt}(\beta) & C'_{Dt}(\beta) - C_{Lt}(\beta) & 0 \\ 2C_{Lt}(\beta) & C_{Lt}(\beta) + C'_{Lt}(\beta) & 0 \\ 2BC_{Mt}(\beta) & BC'_{Mt}(\beta) & 0 \end{bmatrix} \dots\dots\dots (3.22)$$

$$\underline{K}_a = \frac{1}{2} \rho U^2 B \begin{bmatrix} 0 & 0 & C'_{Dt}(\beta) \\ 0 & 0 & C'_{Lt}(\beta) \\ 0 & 0 & BC'_{Mt}(\beta) \end{bmatrix} \dots\dots\dots (3.23)$$

Replacing no and no in equations no yields

$$\underline{M}\ddot{\underline{q}}(t) + (\underline{C} + \underline{C}_a)\dot{\underline{q}}(t) + (\underline{K} + \underline{K}_a)\underline{q}(t) = \underline{F}_r(t) \dots\dots\dots (3.24)$$

Depending on the mean wind velocity and on the variation of shape coefficient, the matrices \underline{C}_a and \underline{K}_a can originate either a stable or an unstable behavior, or even lead to a critical point of bifurcation of the response. The action of wind gust normally leads to stable systems. Instability is caused by the presence of negative terms in the aerodynamic damping matrix and can lead to galloping. The presence of negative coefficients in the stiffness matrix can produce bifurcation. Given the stiffness of structural elements by comparison with aero-elastic stiffness coefficients, this condition is unlikely for civil engineering structures.

3.5. Vibration phenomenon directly induced by wind

3.5.1. Vortex-shedding

Structures shed vortices in a subsonic flow. Vortex shedding is an unsteady flow that takes place in special flow velocities (according to the size and shape of the cylindrical body). In this flow, vortices are created at the back of the body and detach periodically from either side of the body. Vortex shedding is caused when a fluid flows past a blunt object. The fluid flow past the object creates alternating low-pressure vortices on the downstream side of the object. The object will tend to move toward the low-pressure zone. In case of cable-stayed bridges, the slender stay cables can be sufficiently flexible that, in air flow with a speed in the critical range, vortex shedding can drive the stays into violent oscillations that can damage or destroy the bridge.

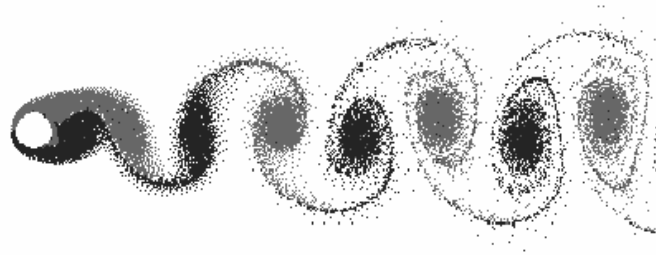


Figure- 3.12. Vortex shedding behind a circular cylinder.

The presence of a circular cylinder in a uniform wind flow has shown that for a very low wind speed the flow detaches from the cylinder and a turbulent wake is generated, characterized by an alternate shedding of vortices at the top and bottom surfaces of the cable. These vortices induce approximately sinusoidal excitation components $f_{D_s}(t)$, $f_{L_s}(t)$ and $m_s(t)$ as defined in expression 3.5. The actuation of the cylinder by these force components generate oscillations, which are normally characterized by very small amplitudes.

In civil engineering applications, the inertial component associated with the added mass of air is normally disregarded in view of its small value. The aerodynamic damping component is, however, of great importance, as negative aerodynamic damping coefficients produce reduced damping force, leading to vortex-induced vibrations. Vortex shedding was one of the causes proposed for the failure of the original Tacoma Narrows Bridge (Galloping Gertie) in 1940, but was rejected because the frequency of the vortex shedding did not match that of the bridge. The bridge actually failed by aero-elastic flutter.

Vortex shedding frequency is given by,

$$f_s = \frac{SU}{D} \dots\dots\dots (3.24)$$

Where, S is the strouhal number, U is the velocity of the wind approaching the stay cable and D is the diameter of the stay cable.

As per IS 875 (Part 3),

$$S = 0.20 \text{ for } bVz \leq 7$$

$$= 0.25 \text{ for } \geq bVz$$

For the Cable-stayed Bridge considered for the present study,

$$b \times Vz = 0.16 \times 47.07 = 7.53$$

Therefore S=0.25

$$f_s = \frac{0.25 \times 47.07}{0.16} = 73.55 \text{ Hz}$$

If some cable frequency is close to f_s of shedding, then a resonance effect takes place, which is known as vortex resonance. The increased oscillation leads the cylinder to interact strongly with the flow and control the vortex-shedding mechanism for a certain range of variation of wind velocity: i.e. an increase of flow velocity by few percent will not change the shedding frequency, which coincides with the natural frequency of the cable. This aero-elastic phenomenon is commonly known as lock-in or synchronization, and produce additional across-wind loads, which are characterized by an inertial component proportional to the accelerations of the structure, and an aerodynamic damping coefficient proportional to the velocity.

3.5.2. Buffeting

Buffeting is high-frequency instability, caused by airflow separation or shock wave oscillations from one object striking another. It is caused by a sudden impulse of load increasing. It is a random forced vibration.

The action of wind gusts on the cable is characterized by the application of drag, lift and moment forces in the along-wind direction, $f_{Du}(t)$, $f_{Lu}(t)$ and $m_u(t)$, and in the across-wind direction, $f_{Dv}(t)$, $f_{Lv}(t)$ and $m_v(t)$, whose linearised form is given by expression no and no, respectively. These expressions show the proportionality of all force components to mean wind speed U and to the fluctuations $u(t)$ and $v(t)$, and hence to the intensity of turbulence.

As an elastic system, the amplitude of the cable response obtained by the solution of turbulence no increases with the growth of buffeting forces, and hence with the mean velocity. However, the growth of wind velocity leads also to increase of aerodynamic damping, as evidenced by the coefficients of the aerodynamic damping matrix \underline{C}_a . The importance of the aerodynamic damping can be analyzed from a simplified modal analysis of a circular cable of diameter D under a smooth flow. For the k_{th} vibration mode, an aerodynamic damping coefficient $\xi_{aero,kD}$, in the along-wind direction is approximated by

$$\xi_{aero,kD} = \frac{\rho U D C_D}{2m\omega_k} \dots\dots\dots (3.25)$$

Where m is the cable mass per unit length and ω_k is the k_{th} order circular frequency. For the across-wind direction, the aerodynamic damping coefficient $\xi_{aero,kL}$ is given by,

$$\xi_{aero,kL} = \frac{\rho U D C_D}{4m\omega_k} \dots\dots\dots (3.26)$$

The relation of 2:1 between the aerodynamic damping coefficients in the along-wind and across-wind direction may contribute to the fact that most vibration problems in cable stayed bridges occur in the plane of the cables.

The significant increase of damping at high wind velocities prevents, most situations, the occurrence of important cable oscillations under buffeting loads.

3.5.3. Galloping

Galloping is an instability phenomenon typically of slender structures with or “D” cross-sections, which is characterized, in a similar manner to vortex-shedding, by oscillations transverse to the wind direction, that can occur at frequencies close to some natural frequency of the structure. The phenomenon is however quite different from vortex –induced vibration. In effect, while the later produces small amplitudes of oscillations in restricted ranges of wind velocity, galloping occurs for all wind speeds above critical value and produces high amplitude vibrations, which may be ten times or more the typical body dimension.

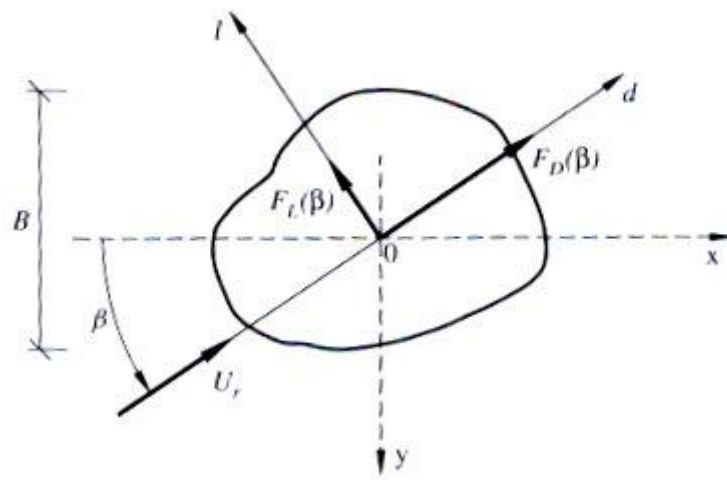


Figure-3.13. Lift and Drag forces on a fixed bluff object.

Consider a section of prismatic body in a smooth occurring flow. Assuming that the body is fixed and that the angle of attack of the flow velocity U_r is β , drag and lift forces $F_D(\beta)$ and $F_L(\beta)$ develop along and across wind direction, respectively, with mean values defined by expressions no and no.

The projections of these two force components on the direction y is then

$$F_y(\beta) = -F_D(\beta) \sin \beta - F_L(\beta) \cos \beta \quad \dots\dots\dots (3.25)$$

Introducing (3.3a) and (3.3b) and (3.3c), the following relation is obtained

$$F_y(\beta) = \frac{1}{2} \rho U^2 B C_y(\beta) \quad \dots\dots\dots (3.26)$$

$$\text{Where, } U = U_r \cos \beta \quad \dots\dots\dots (3.27)$$

And the force coefficient along the vertical direction $C_y(\beta)$ is

$$C_y(\beta) = -[C_L(\beta) + C_D(\beta) \tan \beta] \sec \beta \quad \dots\dots\dots (3.28)$$

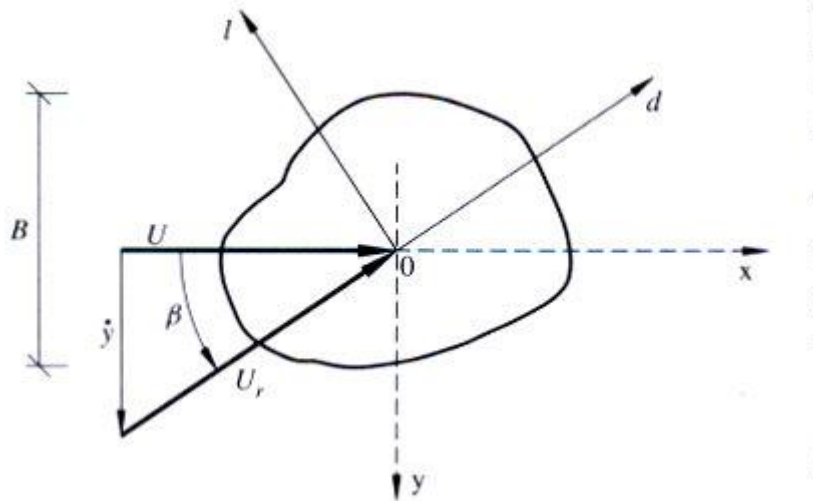


Figure-3.14. Effective angle of attack on an oscillating bluff body.

In the second situation assume that the bluff body is vibrating in the across wind direction y in a flow with velocity U (Fig 3.14)

The relative velocity of the flow with respect to the moving body is obtained from the vector difference represented in (Fig 3.14.) whose amplitude is

$$U_r = \sqrt{U^2 + \dot{y}^2} \dots\dots\dots (3.29)$$

And whose angle of attach is

$$\beta = \tan^{-1} \frac{\dot{y}}{U} \dots\dots\dots (3.30)$$

The dynamic equation of motion of bluff body in the direction is then

$$m\ddot{y} + 2\xi m\omega\dot{y} + m\omega^2 y = F_y(\beta) \dots\dots\dots (3.31)$$

Where m is the mass of the body per unit length, ξ is the damping ratio, ω is the natural frequency of the body

In case of small motion the angle of attach can be neglected, i.e.

$$\beta \approx \frac{\dot{y}}{U} \approx 0 \dots\dots\dots (3.32)$$

So, an expansion of $F_y(\beta)$ about $\beta = 0$ followed by a linearization leads to

$$F_y(\beta) \approx \left. \frac{dF_y}{d\beta} \right|_{\beta=0} \cdot \beta \dots\dots\dots (3.33)$$

Considering that

$$\frac{dF_y}{d\beta} = \frac{1}{2} \rho U^2 B \frac{dC_y}{d\beta} \dots\dots\dots (3.34)$$

And the derivative of the force coefficient C_y with respect to the angle of attack β is

$$\left. \frac{dC_y}{d\beta} \right|_{\beta=0} = - \left(\frac{dC_L}{d\beta} + C_D \right)_{\beta=0} \dots\dots\dots (3.35)$$

Equation.3.31 can be transformed into,

$$m\ddot{y} + 2\xi m\omega\dot{y} + m\omega^2 y = -\frac{1}{2} \rho U^2 B \left(\frac{dC_L}{d\beta} + C_D \right)_{\beta=0} \cdot \frac{y}{U} \dots\dots\dots (3.36)$$

The above equation shows that the aerodynamic force on the bluff body is damping force. This force modifies the overall system damping to a net value d of

$$d = 2\xi m\omega + \frac{1}{2} \rho U B \left(\frac{dC_L}{d\beta} + C_D \right)_{\beta=0} \dots\dots\dots (3.37)$$

The stability of the vibrating cable is guaranteed provided that the viscous damping d is positive. Given the fact that the mechanical damping is always positive, a necessary condition for instability is then

$$\left(\frac{dC_L}{d\beta} + C_D \right)_{\beta=0} < 0$$

The analysis of the expression clearly shows that circular cross-sections are never subjected to instability by galloping, as the derivative $\frac{dC_L}{d\beta}$ is always zero due to symmetry. So except for the case where the external shape has been altered, either by the presence of ice or of water rivulet instability by galloping should not be expected in cable-stayed bridges employing circular cross section for the stays.

In recent studies the instability phenomenon of circular inclined cables has been identified in the laboratory and described as dry inclined cable galloping

3.5.4. Flutter

Cable-stayed bridges are long slender flexible structures which have potential to be susceptible to a variety of types of wind induced vibrations, the most serious of which is the aerodynamic instability known as flutter. At certain wind speeds aerodynamic forces acting on the deck are of such a nature so as to feed energy into an oscillation structure, so increasing the vibration amplitudes, sometimes to extreme levels where the basic safety of the bridge is threatened. The wind speed at which flutter occurs for completed bridges depends

largely on its natural frequencies in vertical flexure and torsion and on the shape of the deck section which determines the aerodynamic forces acting. The Tacoma Narrows Bridge was collapsed because of the flutter phenomenon. For flutter stability, the lowest wind velocity inducing flutter instability of a bridge must exceed the maximum design wind velocity of that bridge.

Wind forces per unit of deck length produced by a steady wind speed U at any location of the bridge deck are usually represented by three components, D (drag), L (lift) and M (moment). The motion dependent aero-elastic forces distributed on unit span of bridge girder are expressed in terms of the displacements and velocities of the bridge deck.

$$\begin{bmatrix} L \\ D \\ M \end{bmatrix} = \frac{1}{2} \rho U^2 (2K^2) \begin{bmatrix} H_4^* & H_6^* & H_3^* \\ P_6^* & P_4^* & P_3^* \\ A_4^* & A_6^* & A_3^* \end{bmatrix} \begin{bmatrix} h \\ p \\ \alpha \end{bmatrix} + \frac{1}{2} \rho U (2BK) \begin{bmatrix} H_1^* & H_5^* & BH_2^* \\ P_5^* & P_1^* & BP_2^* \\ A_1^* & A_5^* & BA_2^* \end{bmatrix} \begin{bmatrix} \dot{h} \\ \dot{p} \\ \dot{\alpha} \end{bmatrix} \dots\dots\dots (3.37)$$

Where,

$\rho =$ air density

B = width of deck

K = reduced frequency

h, p, α = displacement in lift, drag and moment directions respectively

$\dot{h}, \dot{p}, \dot{\alpha}$ = displacement in lift, drag and moment directions respectively

P_i^*, H_i^*, A_i^* = flutter derivatives or aeroelastic coefficient (i= 1 , 2 , , 6)

3.5.5. Wake Effects

Wake effects is the term used for all the vibration phenomenon of stays that lie in the wake of other stays or structural elements, or of some construction equipment. The perturbing element affects the wind flow, creating local turbulent conditions that produce oscillations of the cable. These oscillations may be associated with resonant buffeting, vortex resonance, galloping or other specific phenomenon. Wake oscillation cannot be anticipated in the design phase, the most effective counter-measure being the addition of damping in the cable in order to balance any negative aerodynamic damping.

The most common situations that produce cable vibrations due to wake effects are described below.

3.5.5.1. Resonant buffeting

This phenomenon can occur with two parallel planes of cables. The wind gust strikes the up-wind and down-wind planes of cables with time delay of B/U , B being the distance between the two planes of cables and U the mean wind velocity. If the delay coincides with half the period T_t associated with the torsional deck mode, then resonant effect can be attained.

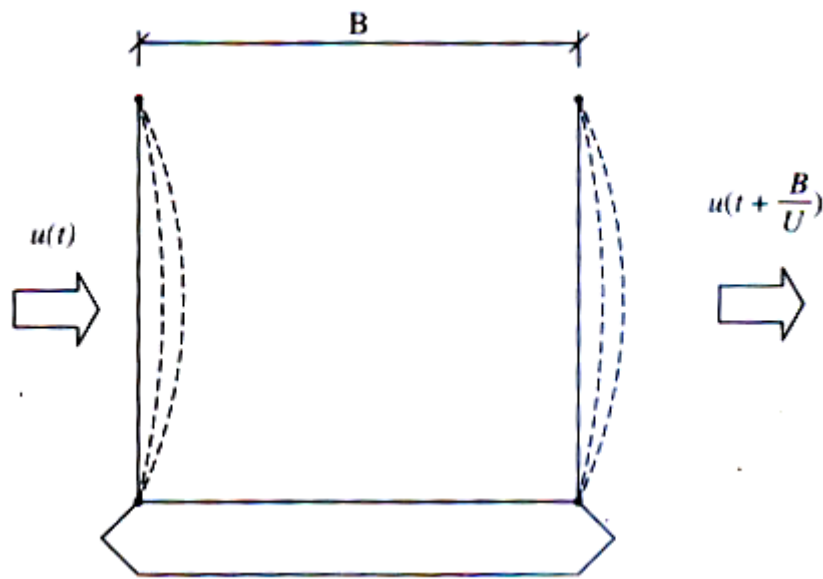


Figure- 3.15. Action of gust on the two planes of stays.

The critical velocity U_{cr} for the resonant buffeting is then defined by

$$U_{cr} = \frac{2B}{T_t} \dots\dots\dots (3.38)$$

3.5.5.2. Vortex resonance

This phenomenon occurs typically in cable-stayed bridges with two planes of cables when subjected to oblique winds. In that case, the wind flow is modified in the wake of the pylon (Fig 3.16), and vortices shed at a frequency defined by

$$f_v = \frac{USt}{B} \dots\dots\dots (3.39)$$

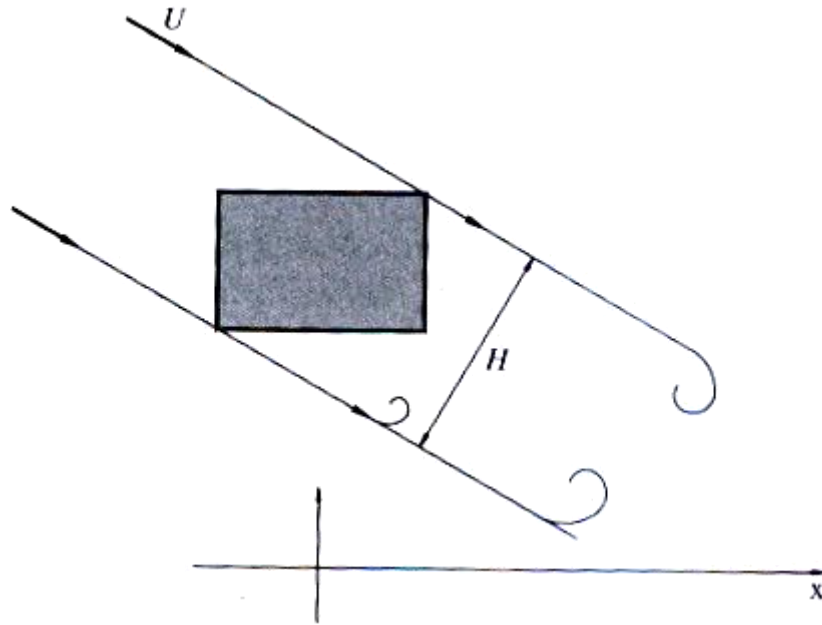


Figure - 3.16. Vortex shedding in the wake of a bridge pylon.

Resonant effects may occur for the cables behind the pylon that have a natural frequency f_k close to shedding frequency. The critical wind velocity U_{cr} for the occurrence of vortex resonance of a cable frequency f_k in the wake of a pylon can therefore be evaluated from

$$U_{cr} = \frac{Hf_k}{St} \quad \dots\dots\dots (3.40)$$

Where, H is the projection of the pylon in the direction transversal to the wind and St is the Strouhal number of the pylon cross section.

3.5.5.3. Interference effects

In order to restrain the size of the cables, multiple parallel stay cables have been used in several cable-stayed bridges. These multiple cables are distant from each other by a few diameters only and are anchored in the tower and deck at the same level.

It has been observed that under particular condition the cable assembly may undergo vibrations. These oscillations are due to vortex resonance to galloping of the cable assembly or to so called interference or wake galloping. The latter phenomenon is no more than a galloping that occurs on the downstream cable(s) induced by the turbulent wake of the upstream cables(s). The oscillation of the downstream cable(s) may induce also a perturbation of the flow around the upstream cables(s), generating oscillations of these cables, designated as interference galloping.

3.6. Rain-wind induced vibrations

Rain/wind-induced vibrations appear to be the most problematic of the measured vibrations, with their large amplitudes and relatively frequent occurrence, and are among the most significant considerations in the design of mitigation measures for stay cables. Rain-induced vibrations of power lines was identified a decade ago, but the exact phenomenon has not been well understood, but some aspects of this complex phenomenon can however be outlined: first, it is under the combined action of rain and wind, at specific angles of attack and intensity of rainfall, that rivulets form at the upper and lower surface of the cable. The formation of that rivulets as the result of the balance of gravitational, aerodynamic and surface capillarity forces, leads to a loss of symmetry of the cable cross section and therefore to a variation of aerodynamic forces on the cable. Eventually a decrease in the drag coefficient and a negative slope of the lift coefficient associated with a small variation of the angle of attack may lead to negative aerodynamic damping, resulting in galloping instability. Once the cable starts oscillating, the rivulets tend to oscillate with same frequency. A coupling of this oscillation with the flexural oscillation of the cable may lead to aerodynamic instability, which is likely to intensify the vibrations.

3.7. Drag Crisis

A recent concern of several researchers is that many wind-induced vibrations have occurred in the critical Reynolds number range. In fact, the critical range of Reynolds number is $2 \times 10^5 - 8 \times 10^5$ for smooth cylinders, meaning that for a circular stay cable of diameter of 0.20m this range would occur for mean wind velocities of 20-60m/s. So, assuming vibration of the cable in that particular range of Reynolds number, a small increase of mean velocity might create sudden decrease of drag force, and hence of lift force over the cable, the result being a reduced motion. This approximation to the equilibrium position would cause an increase of the relative velocity of the flow and so a slight increase of drag force and of cable vibration with consequence of reducing the relative wind velocity of the flow. An oscillation of the cable could then be created merely by a slight fluctuation of wind flow.

The so-called drag crisis has not been truly identified on cable-stayed bridge, although it is currently understood as the source of large oscillations observed in few cable-stayed bridges in UK. It is thought that a Reynolds number in critical range can enhance the generation of rain-wind induced vibration. This phenomenon is quite complex, and depend on the attitude of the circular cylinder to the flow and requires further investigation.

3.8. Indirect Excitation

The vibration of the deck and tower caused by wind, traffic and earthquake, produces an indirect excitation of the cables through the motion of the anchorages. In certain circumstances, the induced cable vibrations attain very high amplitude. Two phenomena can be identified under these circumstances:

1. External excitation
2. Parametric excitation

The literature on indirect excitation concentrates essentially on studies on the parametric excitation phenomenon, which is considered more important; the usual approach to the study of parametric excitation consists of an evaluation of the cable resonance condition from the dynamic equilibrium equations of a single cable under harmonic motion of the supports.

Chapter 4

MODELLING AND ANALYSIS

4.1. General

Cable-stayed bridges are highly complex structures. The accurate structural analysis of cable stayed bridges was very difficult in the past. The static and dynamic analyses of cable stayed bridges require the application of accurate and efficient mathematical models. In most of the previous studies, the stay cables have been modeled with single truss elements; tower and deck were modeled by using frame or beam elements in the finite element analysis. The inadequacy of using single truss elements for cable modeling and recommended the use of multiple elements for each cable. Now, it is no longer a problem to accurately predict the static and dynamic structural behavior of cable stayed bridges. The finite element method provides a convenient and reliable idealization of the structure and is particularly effective in digital computer analysis. The drawback of simplified models was overcome by the commercial analysis codes which have been developed and commonly used in structural analysis in recent years. These commercial codes enabled the modeling of complex civil structures in detail and more accurately with all the components represented by a large number of shell and solid elements. The structural components could be more realistically modeled in the finite element method. The advantage of the finite element method is that, structural complexities such as tower movements, cable extensibility, and support conditions etc. can be considered effectively. In the present report, three dimensional finite element model of a cable-stayed bridge in Indian terrain conditions is prepared using the commercial software MIDAS CIVIL.

4.2. Nonlinearities of Cable Stayed Bridge

The cable stayed bridges are very long; a lot of nonlinearities are introduced into the cable stayed bridges. The nonlinearities that are to be considered while performing the analysis are described below:

4.2.1. Beam – Column Effect

Since, high pretension force exists in the inclined cables, the tower and part of the girder are under a large compressive action; this means that the beam-column effect has to be taken into consideration for girders and towers of the cable stayed bridges. The structural stiffness

matrix for the structure in which members are subjected to axial load is different from the conventional stiffness matrix. In beam – column effect, the lateral deflection and axial force are interrelated such that its bending stiffness is dependent on the element axial forces, and the presence of bending moments will affect the axial stiffness. The effect of axial compression is to reduce the stiffness of the member and to cause greater deformations. Tensile force on the other hand increases the stiffness and reduces the deformations. The beam – column effect can be evaluated by using stability functions.

4.2.2. Cable Sag Effect

The inclined stay cable of cable stayed bridge is generally quite long. A cable supported at its end, under the action of dead load and axial tensile force, it will sag into catenary shape. The axial stiffness of the cable changes with change in sag. When a straight cable element for a whole inclined cable stay is used in the analysis, the sag effect must be taken into account. To consider the sag nonlinearity in the inclined stay cables, it is convenient to use an equivalent straight cable element. For the equivalent straight cable, the initial Young's modulus is replaced with an equivalent modulus of elasticity, which value will be less than the initial modulus of elasticity of the cable. This concept was proposed by Ernst. There are two considerations in determining the equivalent modulus of elasticity of the stay cables depending upon the change in tension for a cable during load increment. If the change in the tension for a cable during load increment is not large; the equivalent modulus of elasticity of the cable to be considered is given by,

$$E_{eq} = \frac{E}{1 + \frac{E(\gamma L)^2}{12\sigma^3}} \dots\dots\dots (4.1)$$

Where

E = Young's modulus of straight cable

γ = specific weight of the cable

L = horizontal length of the cable

σ = tensile stress in cable

If the change in tension for a cable greatly varies during a load increment, the axial stiffness of the cable will significantly change and the equivalent modulus of elasticity over the load increment is given by:

$$E_{eq} = \frac{E}{1 + \frac{AE(\gamma L)^2(T_i + T_j)}{24T_i^2 T_j^2}} \dots\dots\dots (4.2)$$

Where, A is cross sectional area of the cable, T_i and T_j are the initial and final tension in the cable over the load increment. The cable equivalent modulus of elasticity combines both the effects of material and geometric deformations.

The cable sag effect is considered in the current model. The modulus of elasticity is reduced as per the above mentioned relationship to consider the cable sag effect/

4.3. CABLE-STAYED BRIDGE MODEL

4.3.1. General Arrangement:

The cable-stayed bridge considered is an asymmetric bridge having a total span of 520m. The longer span is of 320m and shorter span is of 200m. A-shaped pylon with an overall height of 86.8m and 51m above carriageway supports the structure by means of two planes of stay cables in a semi-fan arrangement. The towers are made up rectangular concrete sections. The main girder consists of beam and slab type concrete section. Cable spacing is 10m along the bridge deck in both the cable-stayed portions. There are 32 pair and 20 pair of cables in longer and shorter cable-stayed portions respectively. A total of 52 pair stays are present with cable length varying from 176.75m to 31m.

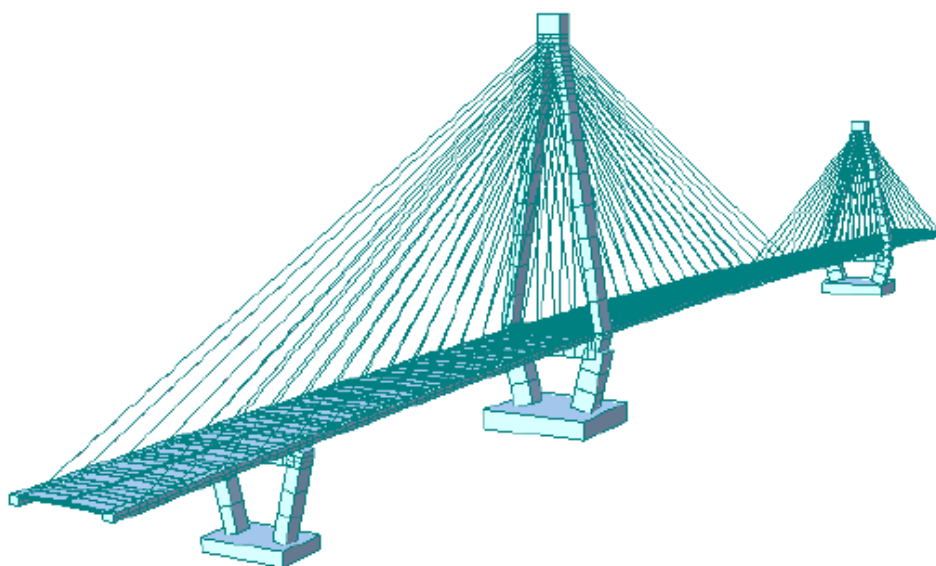


Figure.4.1– Isometric View of the Model

Assumptions in the model:

- i. Stay cables are modeled as truss elements (bending stiffness is null). Also the initial pre-stress is applied initially which are calculated separately by using Unknown load factor method in MIDAS CIVIL.
- ii. The bridge deck, the longitudinal and transverse girders are modeled with equivalent rectangular sections.
- iii. The pylons are modeled as per the geometry as beam elements.
- iv. The general items of the bridge are not modeled in the structure, only the imposed loads are directly modeled.
- v. The foundation structure is not modeled, only the restrains are applied at suitable location.
- vi. The load transfer in transverse direction between two cable planes is done by adding rigid links between the cable anchorages on the either side of the carriageway

4.3.2. Structural Analysis Software:

For the analysis of the cable-stayed bridge, the finite element analysis software MIDAS CIVIL has been used. It has capability of doing large range analysis. Designers can use MIDAS CIVIL for generating bridge models, automated bridge live load, analysis and design, bridge construction sequence analysis, temperature load analysis, large deformation cable supported bridge analysis and pushover analysis. All the above features make MIDAS CIVIL the unique and most appropriate software for the analysis and design of bridges structures.

The wind load analysis has been carried out using the same software. The input calculations for wind loads on the cable-stayed bridge model are done manually. The initial pretension analysis for the same model is carried out using MIDAS CIVIL by using the unknown load factor method. These values of the initial pretension are used as an input for the model used for carrying out modal analysis and wind analysis.

4.3.3. Material:

The total numbers of elements used for creating the model are 1788. These elements were further divided into subgroups, cables, towers, deck, footing, rigid links and supports.

The material that was used in construction of the bridge was M60 Grade of concrete and high tensile steel for stay-cables.

MATERIAL	STEEL
Density	7850 kg/m ³
Young's Modulus	2×10^5 N/mm ²
Poisson's Ration	0.3
MATERIAL	CONCRETE M60
Density	2500 kg/m ³
Young's Modulus	38730 N/mm ² ($5000\sqrt{f_{ck}}$)
Poisson's Ration	0.12

Table 4.1. Material Properties

The geometry was prepared for the model to represent the actual nature of the bridge and appropriate properties were assigned to appropriate elements. The entire bridge after modeling is shown in Figure 1.1. The loading was divided into Dead load, Live load, Pre-stress loads and 2nd dead loads (SIDL). Also the wind loads in transverse direction were applied in a separate load group. The non-linear analysis was carried out for the structure.

4.4. STATIC ANALYSIS

Static analysis of the cable-stayed bridge model has been done considering the dead loads only. For the static analysis under dead loads, the dead load values of various components of the bridge is taken by the software automatically using the volume of the components and the density of the materials assigned to it. MIDAS Civil has large capabilities of static analysis procedure.

Absolute Maximum Values	Vertical Deflection	Along the Deck	Axial Force	Shear Force	Bending Moment
	(m)	(m)	(KN)	(KN)	(KN-m)
Girder	0.34	-	19303	4209	15127
Pylon	-	0.103	76812	550	43989

Table 4.2. Maximum Responses.

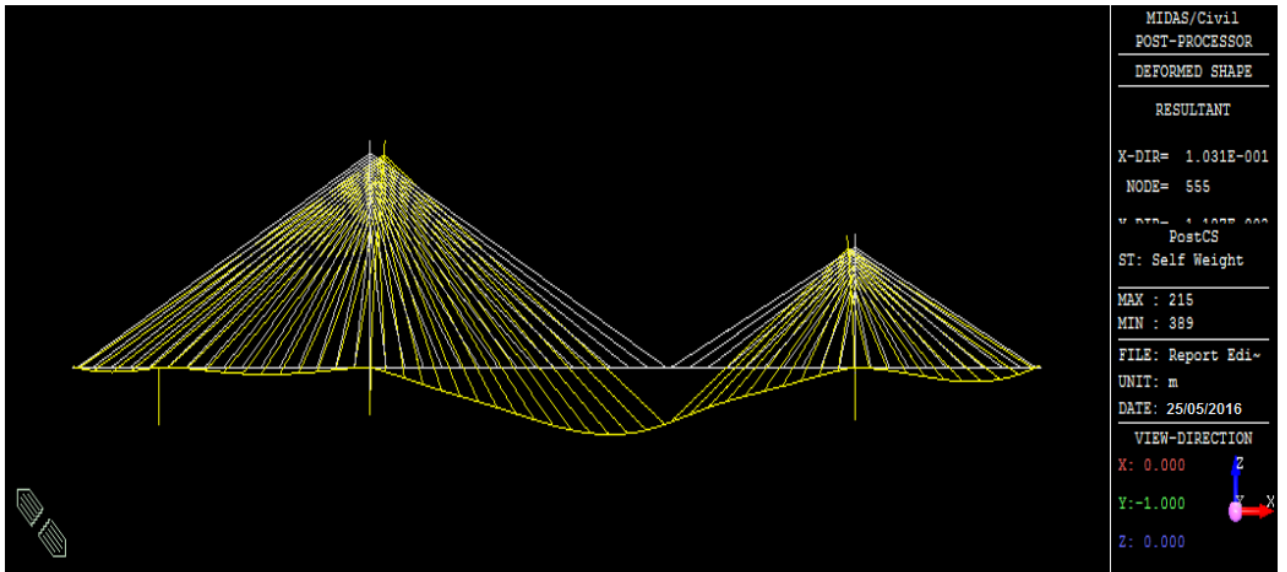


Figure 4.2. Deflection (Dead Load).

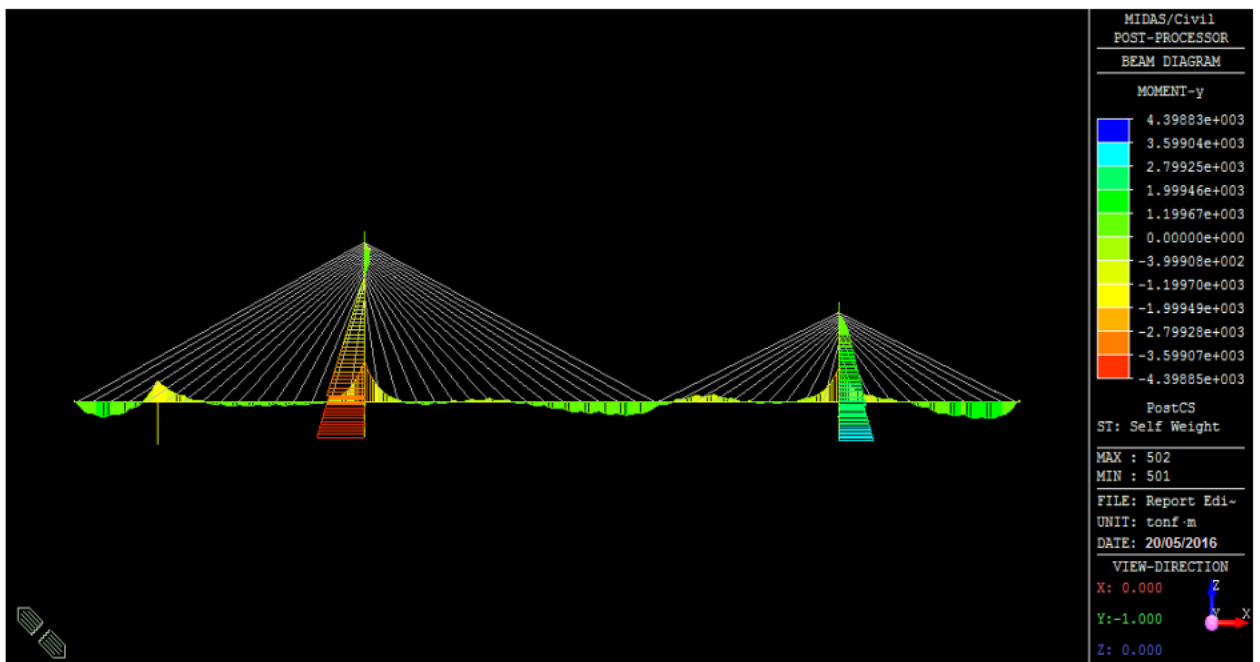


Figure 4.3. Bending Moment Diagram (Dead Load).

4.5. DYNAMIC ANALYSIS

Cable-Stayed bridges are more flexible than other type of bridges because of large spans and relatively slender superstructure. One important aspect of such a flexible structure is large displacement response of the deck when subjected to dynamic loads. As a result, considerable amount of research has been carried out to study the dynamic behavior of cable-stayed bridges as a part of the design of wind and seismic resistance. Seismic analysis has not been carried out for present study. The dynamic characteristics of a structure can be effectively analyzed in terms of natural modes of vibrations i.e. in terms of natural frequencies and mode shapes.

Hence modal analysis is needed to determine the natural frequencies and mode shapes of the entire cable-stayed bridge. The natural frequencies and mode shapes of the entire cable-stayed are studied using the current MIDAS CIVIL model. Since the model is a 3D Finite element model, a general modal analysis capable to provide all possible modes of the bridge (transverse, vertical, torsion and coupled). The natural frequencies and the nature of mode shapes are given in the table 4.3.

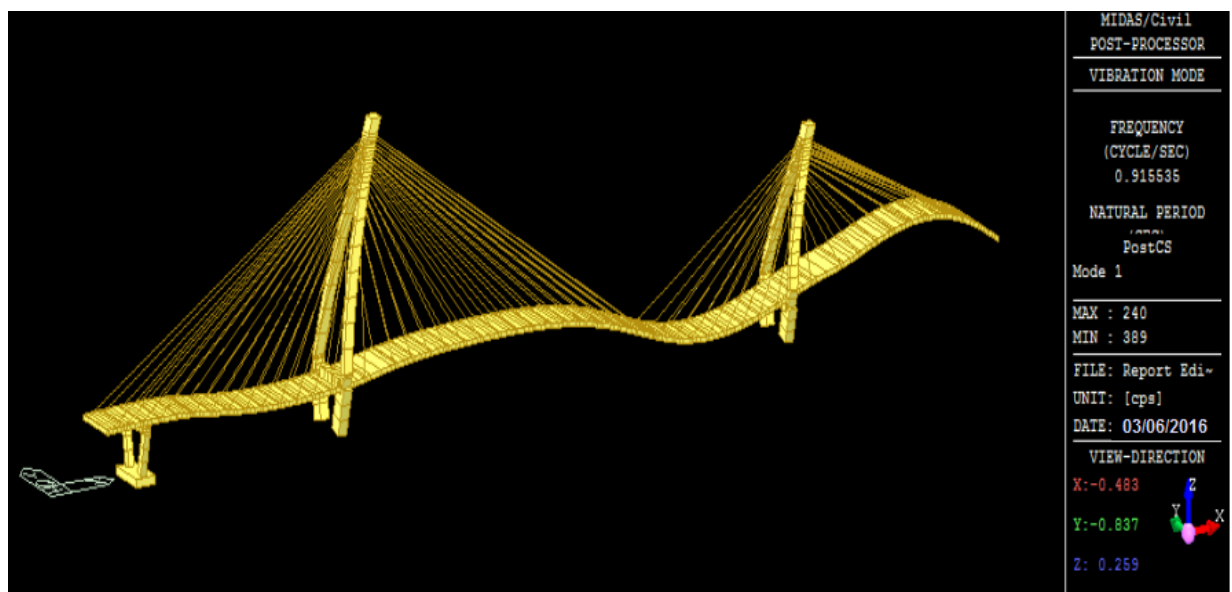


Figure 4.4. 1st Mode Shape- Vertical and Transverse Mode.

Mode No.	Frequency (Hz)	Cumulative Mass Fraction in Given Direction					
		X	Y	Z	Rot X	Rot Y	Rot Z
1	0.92	92.92	0.00	0.03	0.00	0.23	0.00
2	1.18	94.70	0.00	11.41	0.00	0.68	0.00
3	1.56	99.57	0.00	14.06	0.00	3.83	0.00
4	2.33	99.65	0.00	19.94	0.00	4.47	0.00
5	2.45	99.82	0.00	28.22	0.00	27.84	0.00
6	2.69	99.82	28.62	28.22	28.62	27.84	3.04
7	2.69	99.88	28.62	61.15	28.62	39.25	3.04
8	3.00	99.95	28.62	61.78	28.62	49.39	3.04
9	3.42	99.96	28.62	62.84	28.62	54.45	3.04
10	3.67	99.97	28.62	71.60	28.62	54.86	3.04
11	4.20	99.99	28.62	74.18	28.62	61.41	3.04
12	4.30	100.00	28.62	74.35	28.62	66.34	3.04
13	4.53	100.00	28.62	75.53	28.62	66.36	3.04
14	5.34	100.00	28.62	75.53	28.62	69.19	3.04
15	5.78	100.00	28.62	82.99	28.62	74.49	3.04
16	6.25	100.00	59.08	82.99	59.08	74.49	24.65
17	6.54	100.00	59.08	84.40	59.08	75.14	24.65
18	7.11	100.00	59.08	85.78	59.08	81.39	24.65
19	7.68	100.00	64.81	85.78	64.81	81.39	43.11
20	8.00	100.00	64.81	88.14	64.81	81.50	43.11
21	8.17	100.00	64.81	88.37	64.81	81.50	43.11
22	8.64	100.00	64.81	88.49	64.81	82.55	43.11
23	9.62	100.00	64.81	88.51	64.81	83.16	43.11
24	10.99	100.00	64.81	88.53	64.81	83.19	43.11
25	11.47	100.00	64.81	88.95	64.81	83.43	43.11
26	11.80	100.00	87.51	88.95	87.51	83.43	80.28
27	12.09	100.00	87.51	89.97	87.51	84.02	80.28
28	13.14	100.00	87.51	90.56	87.51	84.14	80.28
29	13.40	100.00	87.51	91.03	87.51	85.57	80.28
30	13.71	100.00	92.94	91.50	92.94	87.00	80.32

Table 4.3. Natural Frequencies and Mode shapes.

4.6. CALCULATION OF WIND LOAD

(Gust Factor Method)

The wind on earth’s surface is turbulent in nature that gives rise to randomly varying wind pressures about a certain value associated with the mean wind speed. The dynamic part of the wind pressures would set up oscillations in a flexible structure, which may be defined as one having the fundamental frequency less than 1.0. As seen in the table above, the natural frequency for first mode of vibration is 0.92. Also the height to minimum lateral dimension of the structure considered is greater than 5. Hence the structure is a slender structure. The calculation of the wind load along wind directions have been obtained using Gust factor approach as per IS 875 (part 3) as per Davenport formulation.

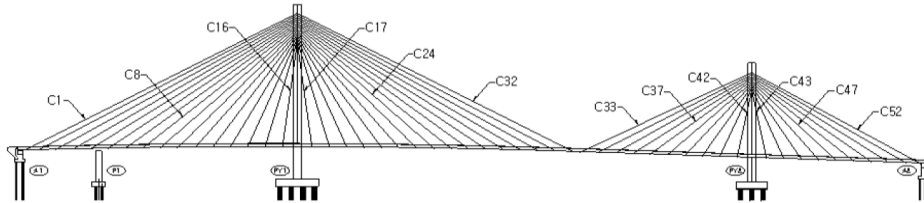


Figure. 4.5. Geometry of Hypothetical Cable-Stayed Bridge

Solidity Ratio

(Refer Table-28, , pg IS: 875 Part (III))

$$C_D = \text{Force coefficient for single plane of Stay Cables} = 1.2$$

(Refer Table-27, pg no. 46 IS: 875 Part (III)) or
(Refer Table-A-1, , pg no.74 IIRC:6 - 2010)

Shielding factor for multiple plane of cables

$$A_{\text{eff}} = \text{Effective area or projected area of the frame normal to wind} = 2179.82 \text{ m}^2$$

$$A_{\text{exp}} = \text{Area enclosed by the boundary of the frame} = 19121.1 \text{ m}^2$$

$$f = \text{Solidity ratio, } f = A_{\text{eff}} / A_{\text{exp}} = 0.11$$

$$C = \text{Centre to centre of frames} = 14.28 \text{ m}$$

$$B = \text{Least overall dimension of the frame normal to the direction of wind} = 81.00 \text{ m}$$

$$b = \text{Spacing ratio, } b = C / B = 0.18$$

$$C_s = \text{Force coefficient depending on spacing ratio} = 0.99$$

b	0	0.18	0.5
f	η		
0.10	1	1	1
0.11	0.99		
0.2	0.9	0.93526	1

Design wind Pressure	(As per cl 209, pg 23, IRC:6-2010)
V_b = Basic wind speed	= 44 m/s
H = The avg. height of exposed surface above the mean retarding surface	= 110 m
V'_z = Hourly mean wind speed (As per Fig.6, pg 24, IRC:6-2010)	= 35.3 m/s
P'_z = Horizontal wind pressure at height H for V_b = 33 m/s	= 747 N/m ²
V_z = Hourly mean wind speed	= 47.0667 m/s
P_z = Horizontal wind pressure at height H = $P'_z \times V_b^2 / 33^2$	= 1328 N/m ² = 0.133 t/m ²

4.6.1. Calculation of Gust Factor (As per Cl.No. 8, IS :875(Part3)-1987)

Gust factor = $\frac{\text{Peak Load}}{\text{Mean Load}}$ and is given by

$$G = 1 + g_f r \sqrt{B(1+f)^2 + \frac{SE}{\beta}} = 1.410$$

To Find out g_{fr} (Refer Fig 8, IS :875(Part3)-1987)

h = Height of structure = 110 m

(IS 875 Cl.No. 5.3.2.1., Category 2 Note)

Terrain category = II

g_{fr} = Refer Fig.8 of IS 875 (part 3) = 0.74

Hourly mean wind speed (Refer Cl.No.8.2., IS :875(Part3)-1987)

V_b = The basic wind speed = 44 m/s

Coefficients :

k_1 = Probability factor (risk coefficient) = 1.07

k_2 = Terrain, height and structure size factor = 1.17

k_3 = Topography factor = 1

$V_h = V_z$ = Hourly mean wind speed at height z
= $V_b \times k_1 \times k_2 \times k_3$ = 55.08 m/s

Size Reduction Factor (S) (Refer Fig .10, IS :875(Part3)-1987)

$$F_0 = \text{Reduced frequency} = \frac{C_z \times f_0 \times h}{V_h} = 21.93$$

where,

f_0 = Natural frequency of the structure = 0.92

C_z = precise data = 12

$$I = \frac{C_y \times b}{C_z \times h} = 3.94$$

where,

C_y = data = 10

b = Breadth of structure normal to the wind stream = 520 m

$$S = \text{Size reduction factor} \quad (\text{Refer Fig 10, pg51, IS :875(Part3)-1987}) \quad = \quad \mathbf{0.01} \text{ m}$$

$$\text{Background Factor (B)} \quad (\text{Refer Cl 8.3, pg50, IS :875(Part3)-1987})$$

$$L(h) = \text{A measure of turbulence length scale Refer Fig9, pg50, IS :875(Part3)-1987} \quad = \quad \mathbf{750}$$

$$\text{Ratio} = C_{zxh} \quad = \quad 1.76$$

$$L(h)$$

$$l = \quad = \quad 3.94$$

$$B = \text{Background Factor} \quad \text{Refer Fig9, pg50, IS :875(Part3)-1987} \quad = \quad \mathbf{0.28}$$

To find f

$$\phi = \frac{g_r \times \sqrt{B}}{4} \quad \text{But zero for category 3 \& } h > 75\text{m} \quad = \quad \mathbf{0}$$

$$\text{Gust energy factor (E)} \quad (\text{Refer Fig 10, pg51, IS :875(Part3)-1987})$$

$$\text{Ratio} = \frac{f_0 \times L(h)}{V_h} \quad = \quad 12.5$$

$$E = \text{Measure of available energy in the wind stream at the natural frequency of the} \quad \mathbf{0.1}$$

$$\text{Damping coefficient} \quad (\text{Refer Table 34, pg52, IS :875(Part3)-1987})$$

$$b = \text{Damping coefficient (As a fraction of critical damping) of the structure} \quad = \quad \mathbf{0.02}$$

Force on each cable is given by ,

$$F_T = P_z \times A \times G \times C_D \times L$$

Where ,

$$P_z = \text{Horizontal wind pressure} \quad = \quad 0.133 \text{ t/m}^2$$

$$A = \text{Area of Cable Projected on plane perpendicular to wind}$$

$$G = \text{Gust Factor} \quad = \quad 1.410$$

$$C_D = \text{Coefficient of Drag} \quad = \quad 1.2$$

Calculations for wind load on each cable are as follows:

Cable No.	Diameter	Length	Area	Total Force on 1st Plane (F_1)	Total Force on 2nd Plane ($C_s \times F_1$)	Force on Each node on 1st Plane of cables	Force on Each node on 2nd Plane of cables
	mm	m	m ²	t	t	t	t
C1	160	177.01	28.32	6.36	6.30	3.18	3.15
C2	160	169.38	27.10	6.09	6.03	3.04	3.02
C3	160	160.05	25.61	5.75	5.70	2.88	2.85
C4	160	150.82	24.13	5.42	5.37	2.71	2.69
C5	115	141.70	16.30	3.66	3.63	1.83	1.81
C6	120	132.71	15.93	3.58	3.54	1.79	1.77
C7	130	123.88	16.10	3.62	3.58	1.81	1.79
C8	130	115.24	14.98	3.37	3.33	1.68	1.67
C9	120	106.84	12.82	2.88	2.85	1.44	1.43
C10	115	98.72	11.35	2.55	2.53	1.28	1.26
C11	110	90.96	10.01	2.25	2.23	1.12	1.11
C12	110	83.62	9.20	2.07	2.05	1.03	1.02
C13	110	76.75	8.44	1.90	1.88	0.95	0.94
C14	110	70.36	7.74	1.74	1.72	0.87	0.86
C15	100	64.04	6.40	1.44	1.43	0.72	0.71
C16	100	54.67	5.47	1.23	1.22	0.61	0.61
C17	100	54.67	5.47	1.23	1.22	0.61	0.61
C18	100	64.04	6.40	1.44	1.43	0.72	0.71
C19	105	70.36	7.39	1.66	1.64	0.83	0.82
C20	105	76.75	8.06	1.81	1.79	0.91	0.90
C21	110	83.62	9.20	2.07	2.05	1.03	1.02
C22	110	90.96	10.01	2.25	2.23	1.12	1.11
C23	120	98.72	11.85	2.66	2.64	1.33	1.32
C24	120	106.84	12.82	2.88	2.85	1.44	1.43
C25	120	115.24	13.83	3.11	3.08	1.55	1.54
C26	125	123.88	15.49	3.48	3.45	1.74	1.72
C27	125	132.71	16.59	3.73	3.69	1.86	1.85
C28	125	141.70	17.71	3.98	3.94	1.99	1.97
C29	160	150.82	24.13	5.42	5.37	2.71	2.69
C30	160	160.05	25.61	5.75	5.70	2.88	2.85

Cable No.	Diameter	Length	Area	Total Force on 1st Plane (F_1)	Total Force on 2nd Plane ($C_s \times F_1$)	Force on Each node on 1st Plane of cables	Force on Each node on 2nd Plane of cables
	mm	m	m ²	t	t	t	t
C31	160	169.38	27.10	6.09	6.03	3.04	3.02
C32	160	177.01	28.32	6.36	6.30	3.18	3.15
C33	160	109.02	17.44	3.92	3.88	1.96	1.94
C34	160	99.49	15.92	3.58	3.54	1.79	1.77
C35	160	90.06	14.41	3.24	3.21	1.62	1.60
C36	160	80.78	12.92	2.90	2.88	1.45	1.44
C37	125	71.71	8.96	2.01	2.00	1.01	1.00
C38	120	62.90	7.55	1.70	1.68	0.85	0.84
C39	115	54.49	6.27	1.41	1.39	0.70	0.70
C40	110	46.60	5.13	1.15	1.14	0.58	0.57
C41	110	39.29	4.32	0.97	0.96	0.49	0.48
C42	105	31.32	3.29	0.74	0.73	0.37	0.37
C43	105	31.32	3.29	0.74	0.73	0.37	0.37
C44	110	39.29	4.32	0.97	0.96	0.49	0.48
C45	110	46.60	5.13	1.15	1.14	0.58	0.57
C46	120	54.49	6.54	1.47	1.46	0.73	0.73
C47	120	62.90	7.55	1.70	1.68	0.85	0.84
C48	125	71.71	8.96	2.01	2.00	1.01	1.00
C49	160	80.78	12.92	2.90	2.88	1.45	1.44
C50	160	90.06	14.41	3.24	3.21	1.62	1.60
C51	160	99.49	15.92	3.58	3.54	1.79	1.77
C52	160	109.02	17.44	3.92	3.88	1.96	1.94

Table 4.3. Maximum Responses.

4.7. WIND ANALYSIS RESULTS

Wind analysis of the hypothetical cable-stayed bridge model has been done considering the wind loads calculated above. For the wind analysis, the wind load values of various components of the bridge are taken from the calculated values above. These loads are introduced as nodal loads at appropriate locations on the Cable-stayed bridge structure.

Absolute Maximum Values	Transverse Deflection (m)	Along the Deck (m)	Shear Force (t)	Transverse Bending Moment (t-m)
Girder	0.00512	-	-	-
Pylon 1	0.0534	-	164.47	2639.39
Pylon 2	0.034	-	71.82	906.39

Table 4.4. Maximum Responses.

Chapter 5

MITIGATION MEASURES FOR WIND INDUCED VIBRATIONS IN CABLE-STAYED BRIDGES

5.1. Introduction

The previous chapters describe the mechanisms which generate the cable vibrations, appropriate counter measures to mitigate the oscillations are described in this chapter. These countermeasures can be implemented at the source, in such a way that the generation of vibration is limited, or at the structure, through the installation of control systems that have the effect of limiting the response.

These measures can be classified broadly into three types:

1. Aerodynamic
2. Structural
3. Mechanical

5.2. Vibration Control Systems

The occurrence of cable vibrations can be prevented or limited by specific operation conditions and maintenance procedure. For the case of indirect vibrations, i.e. vibrations generated by oscillation of the anchorages, possible implementation measures include limiting the number, speed and mass of crossing vehicles and maintenance of the road surface. Other mitigation measures may attempt to modify the shape (aerodynamic control), the mass and stiffness (structural control), or the damping (mechanical control). For indirect oscillations, these measures can be introduced both at the deck and towers, while direct oscillations require the introduction of control systems in cable.

5.2.1. Aerodynamic control of vibrations

The aerodynamic control of vibrations is performed by modifying the cross-sectional configuration. For the bridge deck, some appendages are attached (round fairing, triangular fairings, splitter plates and flaps) to prevent the occurrence of vortices and achieve the streamlining effects.

For bridge towers, either deflector's can be installed, or the corner edges can be cut.

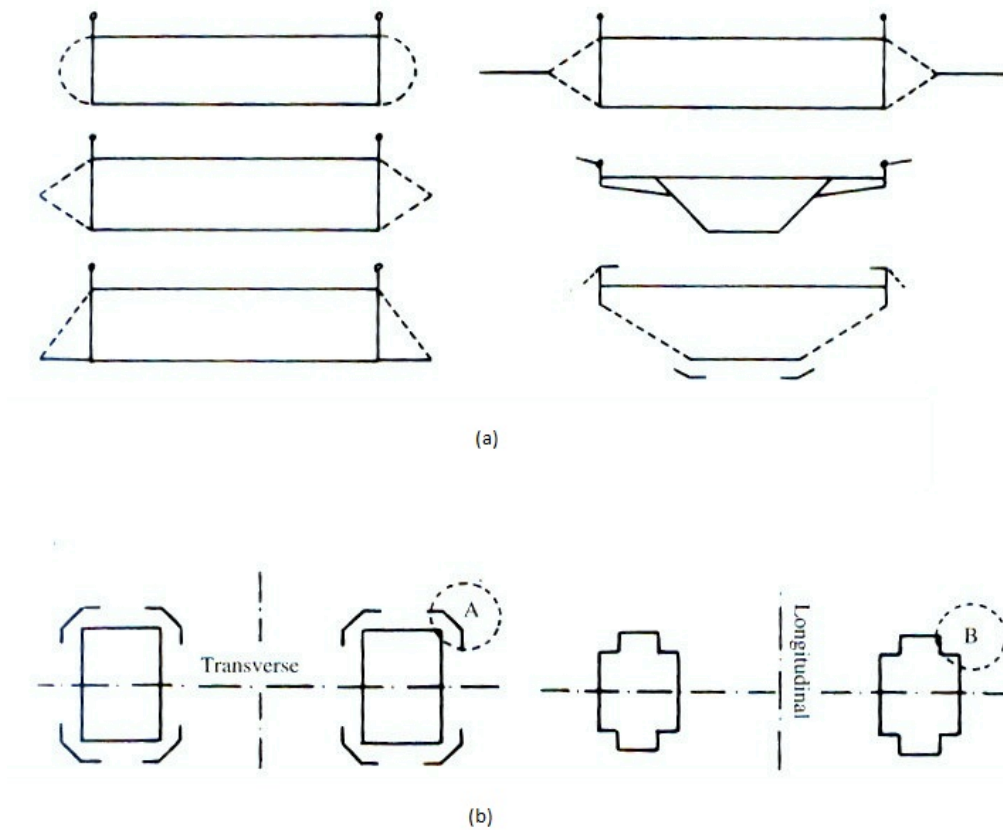


Figure .5.1. (a) – Examples of aerodynamic appendages for a bridge deck.

(b) – Examples of aerodynamic control of vibration for bridge towers

(A: Deflectors B: Corner edge cut)

Although modifications of the shape of cables are limited, the formation of the water rivulets and rain-wind induced vibrations can be prevented by roughening the polyethylene surface of the cable sheath. The main drawback of this procedure is the risk of increasing the drag force for the design for the design wind speed in comparison with the drag force on the normal smooth cable. This aspect is particularly relevant for long span cable-stayed bridges, as the wind load on the cable system is a significant part of overall lateral load. It is however

possible to control the drag forces, if a convenient roughness arrangement is chosen.

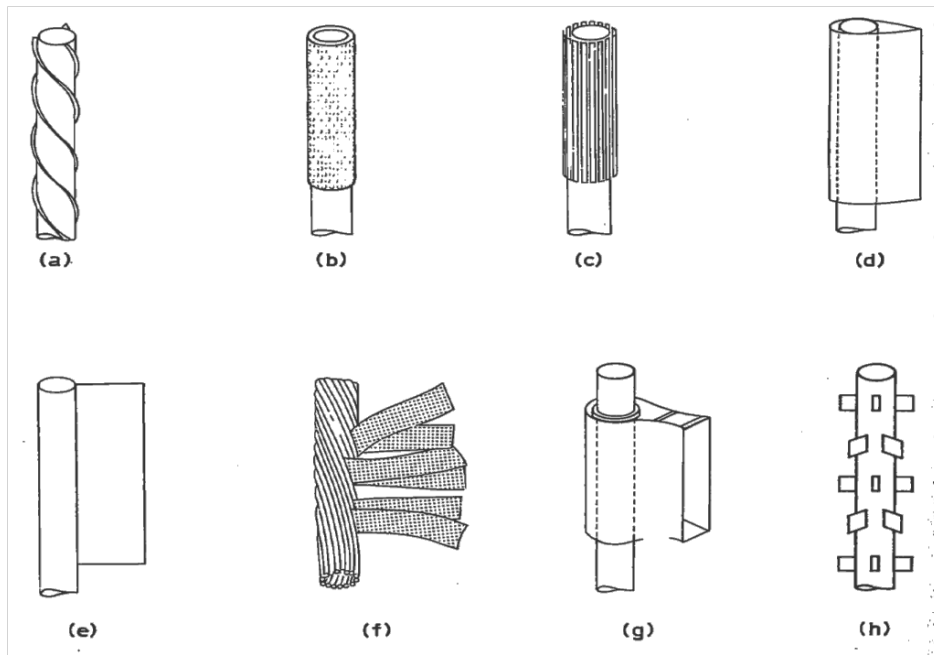


Figure.5.2. Add-on devices for suppression of vortex-induced vibrations:

a) Helical Stake b) Shroud c) axial slats d) streamlined fairing e) splitter f) ribboned g) pivoted guiding vane h) spoiler plate

Another form of aerodynamic control of vibrations consists in adopting a specific cable arrangement. Closely spaced arrangement significantly changes the flow around the cables.

5.2.2. Structural Control of vibrations

Structural control of vibrations by interconnecting ropes has been very frequently used. These interconnecting ropes are often called as crossties. In terms of structural behavior, the addition of cross-ropes to the stay system, creates intermediate support at those elements and consequently increases the natural frequency for vertical vibrations and may be of interest if there is risk of parametric excitation. With a proper design of these ropes (strength, stiffness, prestressing force and connection points of the cross ties), the fundamental frequency of the stay cables is shifted to relatively high values, thus reducing the possibility if internal resonance with global bridge mode shapes. Another significant effect

caused by the installation of cable crossties is an increase in damping.



Figure .5.3. Scheme of cross-cable systems installed some bridges.

However, the initial tension on these cables should have sufficient high value, so that under extreme effects the cross-cables are not detensioned, producing shocks and causing damage to the tie devices. Crossties are effective in the plane of cables only. As the introduction of crossties lower the aesthetic and difficulties in maintenance, other mitigation measures for vibration control are usually adopted.

5.2.3. Mechanical control of vibrations.

The mechanical control of vibrations is achieved by installing damping devices at certain locations along the bridge structure. The low inherent damping capacity of the stay cable can be supplemented by mechanical damping devices (either hydraulic, viscous or friction damping devices). Hydraulic dampers have been used in more recent applications, providing better results. For aesthetic reasons these devices are usually installed near the deck anchorages. The stiffness of the support of these devices should be sufficiently high. A too flexible support will significantly reduce the efficiency of damping devices. Alternative devices for installation either at the bridge towers or inside the bridge deck are the Tuned mass dampers (TMD) and Tuned Liquid Dampers (TLD).

Tuned mass dampers are association of sprung masses (typically 1% to 2% of the overall structure mass) dashpot systems which, when properly tuned and attached at convenient locations along the bridge structure reduce its dynamic response near resonance. The effectiveness of these systems, that were initially used in automobile and aircraft industry. Later these systems were developed for road deck. As shown in (fig.6.3)

Tuned mass dampers can also be installed in stay cables. Although a significant increase of damping can be achieved for the tuned vibration mode. The efficiency of these devices is limited whenever more than one mode of vibration is induced.

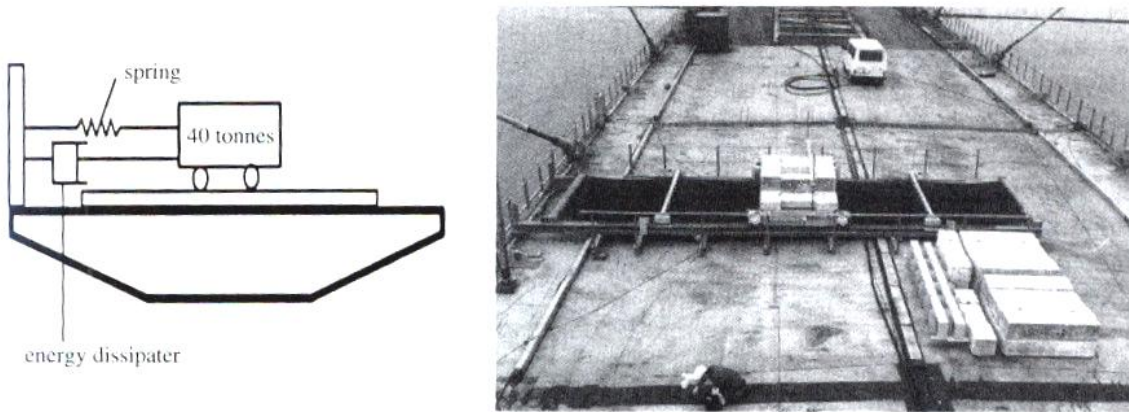


Figure. 5.4.(a) TMD of Normandy bridge, scheme and photograph.

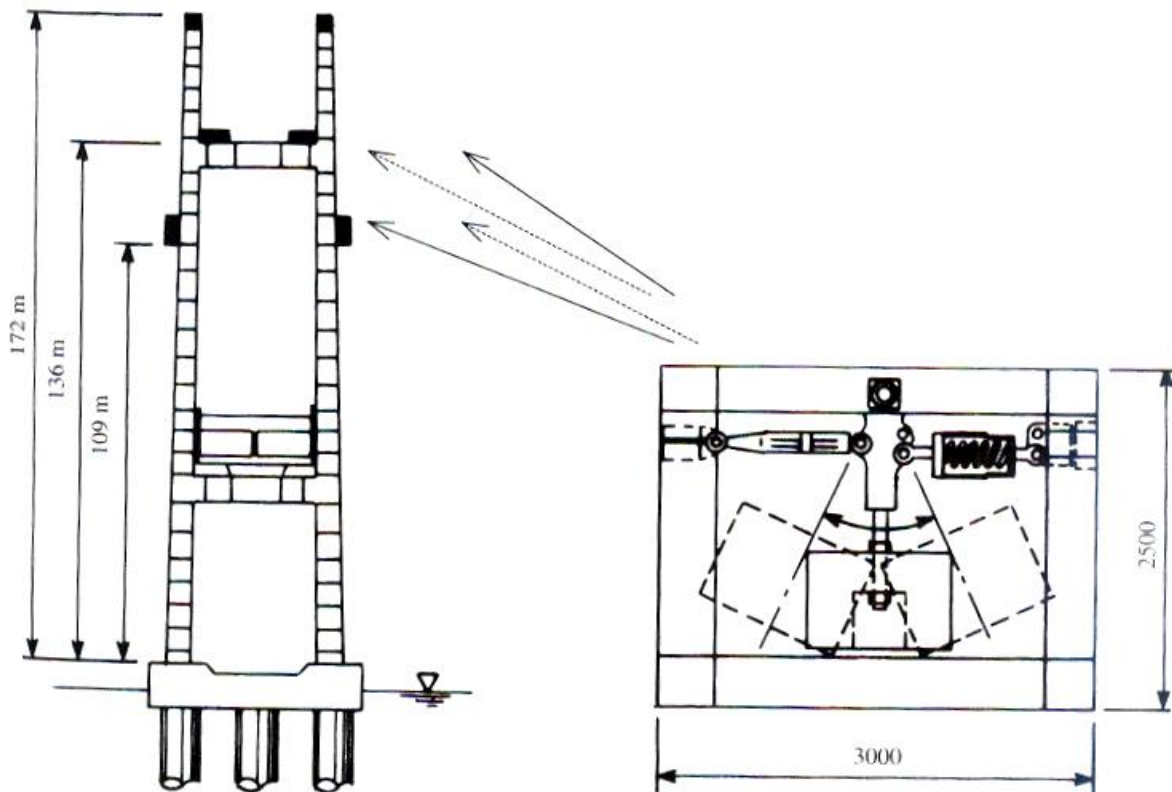


Figure.5.4.(b) Location and scheme of TMDs installed at the towers of Yokhama Bay bridge.

Tuned liquid dampers (TLD) use the motion of liquid inside the container as energy dissipater. Although several applications of these devices are known (mainly for tall

buildings and towers) the physical phenomenon of liquid sloshing motion that reduces the structural response is fully understood, particularly for large amplitude excitations.



Figure.5.5. (a)– Hydraulic damper at Iroise.

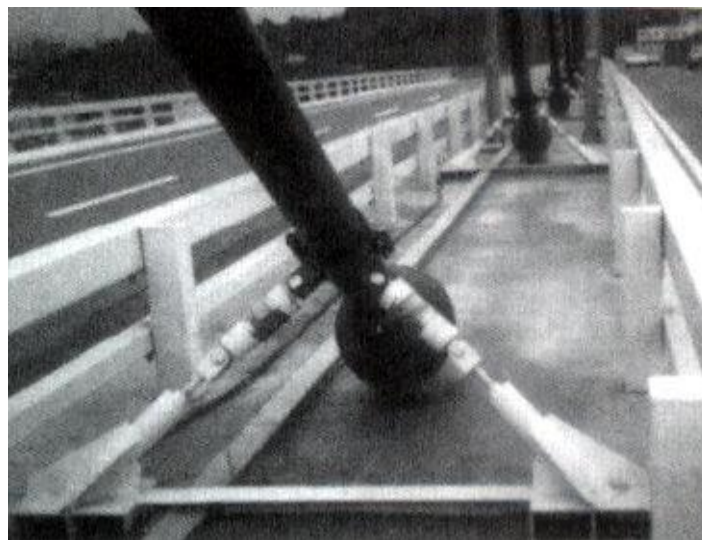


Figure.5.5. (b)– Hydraulic damper at Aratsu bridge.

The installation of hydraulic or viscous dampers close to the stay cables anchorages is a classic and efficient solution for suppressing cable vibrations. The damping capacity of external dampers is defined according to a specified requirement. In general, it is considered that viscous dampers have low maintenance costs, but show a dependence of damping characteristics with temperature and frequency, while hydraulic dampers have high maintenance costs and a complex adjustment. Another reported inconvenience associated with these mechanical devices is the lowering of the aesthetic quality of the bridge.

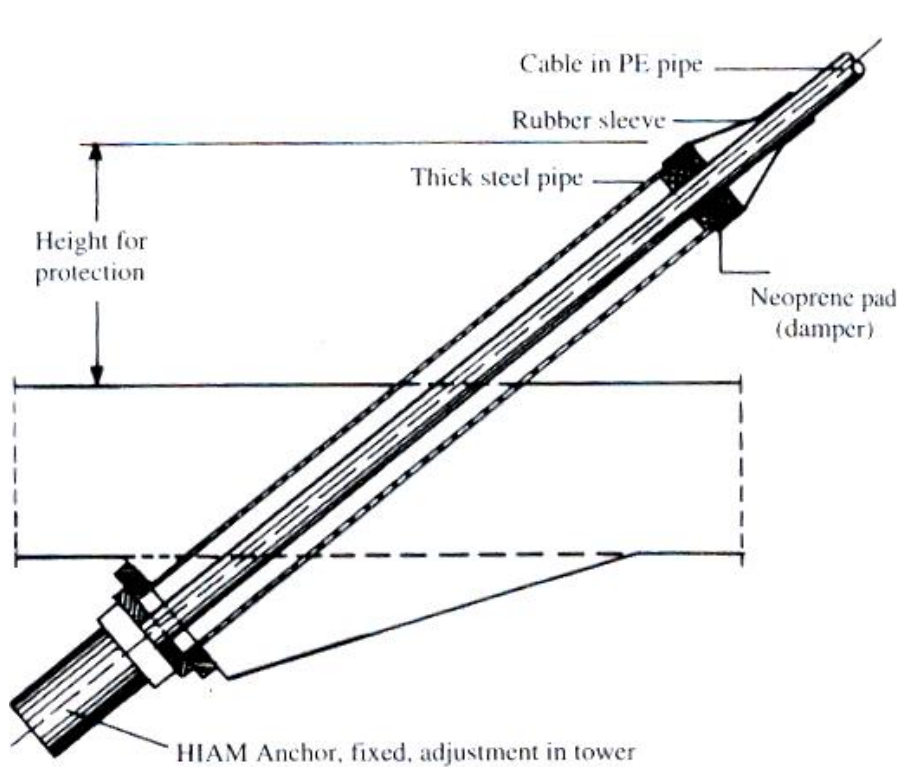


Figure.5.6. Scheme of Ring Damper.

A recent innovation consists in the use of so called internal dampers, which are devices composed by a ring made of neoprene, high damping rubber, or other viscous products placed inside the cable pipe (the deviator guide).

The internal ring dampers need virtually no maintenance and can provide sufficient damping for cables of up to 350m length. The degree of damping depends on the degree of pre-compression in the ring.

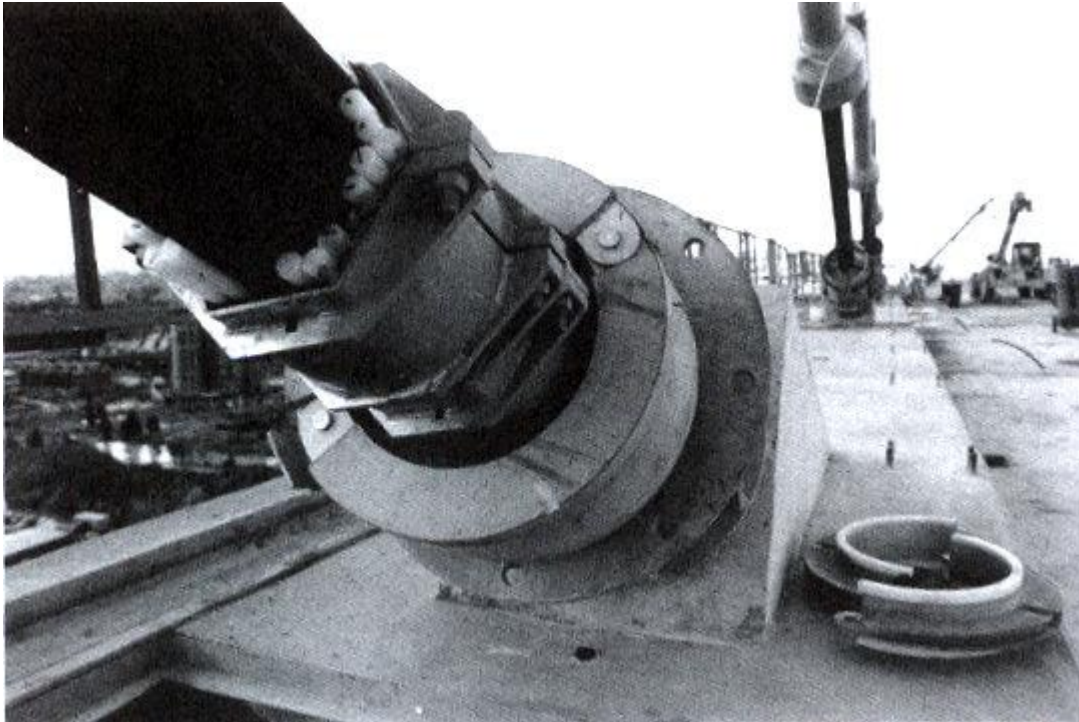


Figure –5.7 – Internal damper installed on a stay cable of Vasco da Gama Bridge.

Finally it is relevant to refer the possibility of increasing cable damping by using adequate grout filler. Studies have shown that Latex filled filler can provide an increase of 60% in damping with respect to conventional cement grout.

5.2.4. Active control system

The basic scheme of active control system includes the following components:

1. Sensors located on the structure for measurement of external excitations and/or structural responses.
2. Devices to process the mechanical information and compute the necessary control forces, according to a specified control algorithm (closed loop, open-loop, or open-closed loop)
3. Actuators, usually driven by external sources.

Basically, the control system can follow two strategies, according to the chosen algorithm, first corresponding to a modification of the structural stiffness and damping so that the structure can respond favorably to the external excitations (closed-loop), and the second, consisting in the reduction or elimination of the external forces (open-loop).

The main active control mechanisms studied for application in the specific domain of bridges are:

1. Active aerodynamic appendages.
2. Tendon control.
3. Active mass dampers.

5.2.4.1. Active aerodynamic appendages

The idea of applying active aerodynamic appendages in ultra-long span bridges was inspired by principles used in the stabilization of surface in the aircraft industry. Two concepts of such types are shown in figure.

The first consist of actively changing the geometry of the side of a streamlined box bridge deck, modifying the flow pattern around the girder to reduce wind-induced excitation. The second consists in the addition of control surfaces attached beneath the edges of the deck by aerodynamically shaped pylons at a consists in the addition of control surfaces attached beneath the edges of the deck by aerodynamically shaped pylons at a convenient distance. The rotation of the surfaces by means of hydraulic actuator produces aerodynamic forces that stabilize the structure, increasing the critical wind speed. Recent studies have shown that a great advantage of this technique of control over the structural methods in the fact that the source of stabilizing forces, the wind, is the same as the source of the aerodynamic sources that cause instability. However, the implementation is very complex, requiring the design of two or three parallel control systems, to ensure that the failure of a controller does not cause the collapse of the bridge.

5.2.4.2. Active tendon control

Active tendon control has been considered as a possible alternative technique to control cable vibrations, particularly for long span cable-stayed bridges, in which the application of passive dampers near the cable anchorage is less effective. Studies in active tendon control have been developed in two-directions: the modal control, which uses the axial motion of the cable-support and the wave-control approach that applies transversal control forces in the cable span support.

5.2.4.3. Active mass dampers

TMDs, which are designed to reduce the response in only one mode of vibration, usually fundamental one. Active Tuned Mass Damper (ATMDs) can be effective over a wide frequency range.

5.3. Summary

Although various mitigation measures for vibration control in Cable-stayed bridges are available the designer must ensure that these means are compatible with the cable stay system and do not impose effects which may be harmful to the behavior of stay cables. Cable-stayed bridges have an inherent aesthetic appeal which should not be lowered by installation of the mitigation measures. Also theoretically the installation of the mitigation measures is very much effective; the mitigation system must be tested and verified on site before and after installation.

Chapter 6

SUMMARY AND CONCLUSION

6.1. Summary

The present study has been conducted to analyse the effects of wind and to understand the various phenomena which cause vibrations in Cable-stayed Bridges. As the study of wind effects is normally conducted by separating the static components and dynamic components associated with the wind, both these components are studied separately. The static analysis is carried out on Cable-stayed bridge for Indian terrain conditions using the Gust Factor Method as per IS: 875 (Part 3) -1987 based on the Davenport's Formulation. All the calculations are done using Microsoft Excel Spreadsheets. The recommendations for wind loads by IRC 6: 2010 are also used.

The static and dynamic analysis of three dimensional finite element model of a cable-stayed bridge in Indian terrain conditions is done using the commercial software MIDAS CIVIL. The dynamic analysis is performed on the same model. Dynamic characteristics of the cable-stayed bridge are analysed effectively in terms of natural modes of vibrations.

6.2. Discussion

The current study presents a brief abstract of wind loads applied to stay cables, concentrating on the effects of the corresponding dynamic components. Particular vibrating phenomena are introduced, namely vortex shedding, buffeting, galloping, flutter, wake effects, rain-wind induced vibrations, and indirect excitations. Also a vibrating phenomena that has been recently identified i.e. Drag Crises is also briefly discussed. A brief context of the mechanisms that govern this phenomenon is explained with regards to the current theories. Various mitigation measures for vibrations in Cable-stayed bridges are discussed in the present study.

6.2. Conclusions

Based on the study carried out in the present work following conclusions are derived:

1. It is evident from the present study that Finite Element Analysis of Cable-stayed Bridges subjected to dynamic loads gives realistic estimate of structural (Shear Force, Bending Moment, Axial Force and Deflection) compared to response obtained using available empirical formulation.
2. The consideration of non-linearities (geometric as well as material) in the analysis of Cable-stayed Bridges is must as their effects on the structural responses is significant and govern the design.
3. As the lowest natural frequency of Cable-stayed Bridge structure is very less (i.e. < 1 Hz) it is necessary to carry out the investigations for Wind induced vibrations.
4. The Analysis of the Cable-stayed Bridges subjected to Wind induced vibrations shows that the structure is subjected to combination of two or more wind induced vibration phenomena simultaneously. The Modal analysis results show many closely spaced and coupled modes.
5. Finite Element Analysis results of Cable-stayed Bridge concur the codal requirement of IS 1893: 2002 that frequency of 90% modal mass contributing modes is less than 33Hz.
6. For Short Span Bridges (i.e. Spans < 30 m), wind loading does not govern the design.
7. For Medium Span Bridges ($30\text{m} < \text{Spans} < 120$ m) only the design of substructure is governed by wind loading.
8. For Cable-Stayed Bridges (Long Span Bridges), the Wind loads govern the design for super-structure and sub-structure.

6.2. Future Scope of work.

The present study can be extended further with following topics:

1. Wind tunnel testing of scaled model of Cable-stayed Bridge.
2. Non-linear static analysis of the bridge with control systems can be carried out to assess the seismic response of the Cable-stayed Bridge.
3. Construction stage analysis of Cable-Stayed bridges.
4. Experimental study for verification of mitigation measures for vibration control in Cable-stayed bridges.

REFERENCES

1. Troitsky, M.S., 1988, Cable-Stayed Bridges: Theory and Design. BSP Professional books, London.
2. Walter. Podolny., and John. B. Scalzi., 1999 , Construction and Design of Cable-Stayed Bridges., John Wiley and Sons, New York.
3. R.Walther., B. Houriet., W. Isler., P. Moia., and J. E. Klein., 1999, Cable Stayed Bridges., Thomson Telford Publishing, London.
4. Belvins. R. D., 2001, Flow Induced Vibrations, Kreiger Publishing Company, Florida.
5. CEB- FEB Bulletin 30., Acceptance of stay cable system using prestressing steel, 2005.
6. Niels J. Gimsin., 1998, Cable Supported Bridges: Concept and Design, John Wiley and Sons, New York.
7. U.S. Department of Transportation, Federal Highway Association, 2007, Wind Induced Vibrations of Stay Cables.
8. Indian Road Congress, IRC:6 2010, 2010, Standard Specification and Code of Practice for Road Bridges.
9. Bureau of Indian Standards, 2000, IS:456 2000, Plain and Reinforced Concrete – Code of Practice.
10. B. N. Sun, Z. G. Wang, J. M. K and Y. Q. Ni., “Cable oscillation induced by parametric excitation in Cable-stayed bridges”.
11. M. S. Pfei and R. C. Batist (1995), “Aerodynamic stability analysis of cable stayed bridges”, Journal of Structural Engineering.
12. Jin Cheng, Jian-Jing Jiang, Ru-Cheng Xiao, Hai-Fan Xiang (2002), “Advanced aerostatic stability analysis of cable-stayed bridges using finite-element method”, Computer and Structure.
13. Nicholas P. Jones and Robert H. Scanlan (2001), “Theory and full bridge modeling of wind response of cable supported bridges”, Journal of Bridge Engineering, Vol-6, No.6, Nov/Dec 2001.